Influence of environment induced correlated fluctuations in electronic coupling on coherent excitation energy transfer dynamics in model photosynthetic systems

Cite as: J. Chem. Phys. **136**, 115102 (2012); https://doi.org/10.1063/1.3693019
Submitted: 30 December 2011 . Accepted: 22 February 2012 . Published Online: 15 March 2012

Pengfei Huo, and David F. Coker

Influence of environment induced correlated fluctuations in electronic coupling on coherent excitation energy transfer dynamics in model photosynthetic systems

Pengfei Huo[1,2] and David F. Coker[1,3,a)]
[1]*Department of Chemistry, Boston University, 590 Commonwealth Avenue, Boston, Massachusetts 02215, USA*
[2]*Division of Chemistry and Chemical Engineering, California Institute of Technology, Pasadena, California 91125, USA*
[3]*Department of Physics, and Complex Adaptive Systems Laboratory, University College Dublin, Dublin 4, Ireland*

(Received 30 December 2011; accepted 22 February 2012; published online 15 March 2012)

Two-dimensional photon-echo experiments indicate that excitation energy transfer between chromophores near the reaction center of the photosynthetic purple bacterium *Rhodobacter sphaeroides* occurs coherently with decoherence times of hundreds of femtoseconds, comparable to the energy transfer time scale in these systems. The original explanation of this observation suggested that correlated fluctuations in chromophore excitation energies, driven by large scale protein motions could result in long lived coherent energy transfer dynamics. However, no significant site energy correlation has been found in recent molecular dynamics simulations of several model light harvesting systems. Instead, there is evidence of correlated fluctuations in site energy-electronic coupling and electronic coupling-electronic coupling. The roles of these different types of correlations in excitation energy transfer dynamics are not yet thoroughly understood, though the effects of site energy correlations have been well studied. In this paper, we introduce several general models that can realistically describe the effects of various types of correlated fluctuations in chromophore properties and systematically study the behavior of these models using general methods for treating dissipative quantum dynamics in complex multi-chromophore systems. The effects of correlation between site energy and inter-site electronic couplings are explored in a two state model of excitation energy transfer between the accessory bacteriochlorophyll and bacteriopheophytin in a reaction center system and we find that these types of correlated fluctuations can enhance or suppress coherence and transfer rate simultaneously. In contrast, models for correlated fluctuations in chromophore excitation energies show enhanced coherent dynamics but necessarily show decrease in excitation energy transfer rate accompanying such coherence enhancement. Finally, for a three state model of the Fenna-Matthews-Olsen light harvesting complex, we explore the influence of including correlations in inter-chromophore couplings between different chromophore dimers that share a common chromophore. We find that the relative sign of the different correlations can have profound influence on decoherence time and energy transfer rate and can provide sensitive control of relaxation in these complex quantum dynamical open systems. © *2012 American Institute of Physics*. [http://dx.doi.org/10.1063/1.3693019]

I. INTRODUCTION

The results of two-dimensional nonlinear spectroscopy experimental studies show the signature of long lived quantum coherent dynamics in a wide variety of nano-structured systems involving chromophores embedded in polymeric scaffoldings such as photosynthetic light harvesting systems[1–5] and conducting polymers.[6] One of the first experimental papers reporting this phenomenon in the chromophores around a chemically modified reaction center model suggested that the mechanism for this long lived coherence[1] involved collective motion in the nano-structured environment that led to correlated fluctuations in chromophore excitation energies. This mechanism for coherent electronic excitation energy transfer has also been suggested in studies on DNA,[9,10] and a similar mechanism has been shown to be operative for coherent vibrational excitation energy transfer in various model systems.[7,8] Scholes and co-workers[2] have suggested that in certain light harvesting complexes such as PC645 or PE545 from cryptophyte algae where the chromophores are covalently bonded to the protein backbone, this type of correlation might be larger compared to regular harvesting complexes in which the chromophores simply intercalate into the protein structure.

Recent molecular dynamics (MD) simulation studies on the Fenna-Mathews-Olsen (FMO) excitation energy transfer network,[11,12] the light harvesting complex 2 (LHII) photosynthetic light harvesting complex[13] and the reaction center complex,[14] however, show no significant correlation in site energy fluctuations after averaging, and similar findings have been reported from calculations for the PE545[15] light harvesting system. However, Kleinekathöfer and co-workers,

a)Electronic mail: coker@bu.edu.

for example, have found that in FMO,[11] there is evidence of correlations in fluctuations of site energy and inter site electronic couplings and electronic coupling-electronic coupling correlations that are more significant compared to the apparently uncorrelated site energy fluctuations. There have been questions raised in recent work about the magnitudes of the parameters used, and the assumptions underlying some of these model calculations.[12,14] There have also been suggestions that the mechanism by which correlated fluctuations in site-energies average out is dynamically more subtle, occurring through the washing out of correlated and anti-correlated site energy fluctuations at different frequencies.[12] The goal of this paper, however, is to study the qualitative characteristics of a different class of models that have received little attention. This paper will thus systematically explore the influence of correlations involving electronic couplings on the quantum dynamics in a model for excitation energy transfer processes between the accessory chlorophyll (Bchl or B) and pheophytin (Bphy or H) in the bacterial reaction center of *Rhodobacter sphaeroides*,[1] the system that was the subject of the early experimental studies where coherent excitation energy transfer was observed by Fleming and co-workers mentioned above. We also present results exploring the effects of such correlations on the population transfer and coherence in a simplified three state model of the FMO light harvesting complex.

There is a rich literature exploring various models for correlated environmental fluctuations.[16–22] Detailed system-bath interaction models have also been developed including a cross-coupling model[23] and the common bath coupling model.[8,9,24–26] All of these studies so far incorporate the effects of correlation between fluctuations in the excitation energies of different sites. As suggested above, other possible correlations between site energy and inter-site coupling fluctuations may be considered. The possible origin of such correlations could be bath modes that influence the relative distances, and angles between two transition dipoles of different chromophores.[27] Some MD simulations suggest that correlated fluctuations in electronic coupling between chromophore dimer pairs that share a common chromophore,[11] for example, correlation between 4–5 coupling and 5–7 coupling in the FMO complex (i.e., inter-site coupling-inter-site coupling correlations) may be significant and one of the primary goals of this paper is to explore the effects of such correlation on the quantum dynamics of model chromophore networks. The simplified systems we explore in this paper thus include both a two state model where we can single out the effects of site energy-inter-site coupling correlations, and a three state example that is a minimal model in which inter-site coupling-inter-site coupling correlation can be explored.

Chen and Silbey[28] and others[29] recently used an extended Haken-Strobl-Reineker (HSR) model that not only includes the site energy correlations but also the site energy-inter-site electronic coupling correlations to study the influence of different types of correlation for a simple two state model. Their work[28] clearly shows that if we also include the effect of the correlation between inter-site electronic coupling fluctuation[27] and site energy fluctuation, the coherent nature of the excitation energy transfer dynamics can be strongly enhanced or suppressed depending on the sign of these correlations. Further, Jang[27] also showed that if an independent bath is coupled to the off-diagonal element in a two state model, this will always enhance the excitation energy transfer rate (assuming that the bath only influences the distance between the two dipoles). Coalson and co-workers[30] recently used the polaron transformation to study the non-Condon effect on a model electron transfer process by including the possibility that the environmental bath can also couple to the off-diagonal element in the spin-boson problem. This study addresses essentially the same type of question as the influence of the bath on the off-diagonal coupling in the excitation energy transfer model described by Chen and Silbey,[28] however, Coalson and co-workers neglected the possibility that the relative sign of the off-diagonal coupling can profoundly change the dynamics.

In this work, we evolve the quantum dynamics of the full multi-chromophore light harvesting system coupled, via various bi-linear interaction models of increasing complexity, to different sets of harmonic bath modes. The approach we employ to perform these large scale dissipative open quantum system simulations is our recently developed approximate semi-classical approach that linearizes the density matrix evolution in the difference between forward and backward paths of the environmental degrees of freedom (DOF)[31,32] while keeping interference effects between forward and backward paths of the system DOF.[33] This new approach is known as the partial linearized density matrix (PLDM) dynamics scheme[34] and it is a highly efficient variant of our earlier iterative linearized density matrix (ILDM) propagation method.[35–37] The PLDM propagation approach is outlined in Sec. S.1 of the supplemental materials for this article.[39] In this paper this approximate quantum dynamics scheme is employed to study the effects of correlations between fluctuations in site energies and inter-site electronic couplings on coherent excitation energy transfer dynamics in a two state reaction center model and a three state excitation energy transfer network. These quantum propagation methods do not suffer from the limitations of the approximations inherent in many traditional approaches such as Foerster Resonant Energy Transfer (FRET) theory[38] and the Redfield or Lindblad equations,[40] or the HSR model for dynamics that assumes infinite temperature and cannot accurately capture finite temperature equilibration at longer times. The new partial linearized version and ILDM propagation approaches have been used[36] to conduct benchmark comparisons with results from various other methods[41,42] and have been shown to be very reliable for a wide variety of applications. Particularly important features of these new methods are their general applicability to arbitrary non-Markovian system-bath spectral densities and beyond bi-linear coupling models. Also these methods are non-perturbative, enhancing their applicability to a diverse range of problems. The trajectory implementation, particularly in the case of the PLDM propagation approach, makes this method extremely numerically efficient.

In this paper, we employ these approaches to study generalized non-Markovian models. Nevertheless, the results of our studies suggest that the findings from the approximate theoretical calculations of Chen and Silbey are gen-

eral and robust. In particular we find that the correlation between site energy and off-diagonal inter-site coupling, and inter-site-inter-site coupling correlations can either enhance or suppress the survival of coherence and the excitation energy transfer rate depending on the type of correlation (positive or negative correlation) just as Chen and Silbey find with their approximate calculations on simplified models. In another calculation on a three state model for FMO we explore various possible correlations, and find that the excitation energy transfer rate is strongly influenced by the relative sign of the correlations, and the same is true for the magnitude of the long lived coherent oscillations in off-diagonal density matrix elements. Further, with these types of correlated fluctuations the trends in the excitation energy transfer rate are not significantly effected relative to the magnitude and decay time of the coherence, which means that for bigger coherence compared to the independent bath model, the exciton transfer rate could be faster or slower, and for smaller coherence, the transfer rate could also be bigger or smaller, depending on the relative sign of the different types of correlations. These studies thus suggest that if these types of correlated fluctuations are operative, the observed coherent dynamics in the experiments is unlikely to play a significant role in the mechanism for excitation energy transfer in these systems, as its presence does not point especially to enhancement of energy transport processes.

II. MODEL SYSTEMS

The experimental results[1] that motivate our first set of model studies were performed on chromophores embedded in the transmembrane protein scaffolding near the reaction center of *Rhodobacter sphaeroides*. In these experiments the primary electron donor (the special pair) is chemically oxidized, shutting down the electron transfer[43] so that only excited state energy transfer between the accessory bacteriochlorophyll (Bchl or B) and bacteriopheophytin (BPhy, or H) is possible. The 2D photon echo experiments by Lee *et al.*[1] showed a long lived beating signal associated with $|H\rangle\langle B|$ coherent dynamics. These authors found that they could fit this spectral dynamics reasonably by assuming the fluctuations in the B and H site energies were strongly correlated, and suggested that in-phase energy fluctuations could be responsible for preserving coherence.[1] It was found that strong electronic coupling, which could also lead to longer lived coherence, would not, however, give a reasonable fit to experimental data.[1] We explore their correlated site energy fluctuation model in detailed calculations presented in Appendix. Below, however, we present an alternative model Hamiltonian that includes correlated fluctuations between chromophore excitation energies and electronic couplings that we show can equally well reproduce the underlying density matrix dynamics probed in the experimental signals.

A. A model Hamiltonian for correlated fluctuations in chromophore excitation energies and inter-chromophore electronic couplings

The model system Hamiltonian that has been determined by fitting the experimental data for coherent excitation energy transfer dynamics between the H and B chromophores in the chemically modified reaction center model is presented in complete detail below, and in Appendix.[1] In addition to variations on the three components outlined here, this experimentally determined Hamiltonian includes a Brownian oscillator mode that modulates the excitation energy of the acceptor state $|B\rangle$. This modulation is important to reproduce the different oscillatory features observed in the experimental signals, in particular the low frequency modulation as we show in Appendix. For the purpose of exploring the factors that influence the electronic quantum coherent dynamics, however, the Brownian mode is a complication that we omit in these studies of the influence of correlated fluctuations in the site and coupling terms.

Here we focus only on the electronic subsystem, bath, and system-bath coupling terms and assume the total Hamiltonian has the following form:

$$\hat{H} = \hat{H}_s + \hat{H}_{s-b} + \hat{H}_b, \tag{1}$$

where the electronic part of the Hamiltonian is

$$\hat{H}_s = \begin{pmatrix} \epsilon_H & \Delta^{(0)}_{HB} \\ \Delta^{(0)}_{BH} & \epsilon_B \end{pmatrix} = \begin{pmatrix} 680 & 210 \\ 210 & 0 \end{pmatrix}, \tag{2}$$

and all the parameter values are given in cm^{-1}. In this section, we explore the situation in which the inter-site off-diagonal coupling bath and the bath that causes fluctuations in site energies are correlated. For simplicity, we assume that all the modes that couple to $|H\rangle\langle H|$ and $|B\rangle\langle B|$ also couple to $|H\rangle\langle B|$ and $|B\rangle\langle H|$. However, the modes coupled to $|H\rangle\langle H|$ and the modes coupled to $|B\rangle\langle B|$ are independent. With the above assumption, the bi-linear system-bath and harmonic bath Hamiltonians can be written as

$$\begin{aligned} \hat{H}_{s-b} &= U^{HH} + U^{BB} + [U^{HB} + U^{BH}] \\ &= \sum_{l=1}^{n^{(H)}} c_l^{(H)} \hat{q}_l^{(H)} |H\rangle\langle H| + \sum_{l=1}^{n^{(B)}} c_l^{(B)} \hat{q}_l^{(B)} |B\rangle\langle B| \\ &\quad + \left\{ k^{(H)} \sum_{l=1}^{n^{(H)}} c_l^{(H)} \hat{q}_l^{(H)} + k^{(B)} \sum_{l=1}^{n^{(B)}} c_l^{(B)} \hat{q}_l^{(B)} \right\} \\ &\quad \times [|H\rangle\langle B| + |B\rangle\langle H|] \end{aligned} \tag{3}$$

and

$$\begin{aligned} \hat{H}_b = \hat{H}_b^H + \hat{H}_b^B &= \sum_{l=1}^{n^{(H)}} \frac{1}{2} \left[\hat{p}_l^{(H)^2} + \omega_l^{(H)^2} \hat{q}_l^{(H)^2} \right] \\ &\quad + \sum_{l=1}^{n^{(B)}} \frac{1}{2} \left[\hat{p}_l^{(B)^2} + \omega_l^{(B)^2} \hat{q}_l^{(B)^2} \right], \end{aligned} \tag{4}$$

respectively, and $[\hat{H}_b^H, \hat{H}_b^B] = 0$, due to the independence of different chromophore baths. With this model, $k^{(B)}$ and $k^{(H)}$ simply modulate the strength with which the independent $\{\hat{q}_l^{(B)}\}$ and $\{\hat{q}_l^{(H)}\}$ bath degrees of freedom influence the inter-site off-diagonal electronic coupling. The assumed form of the bath coordinate dependent electronic coupling with this

model is thus,

$$\Delta_{HB}\left(\{\hat{q}_l^{(H)}\},\{\hat{q}_l^{(B)}\}\right)=\Delta_{HB}^{(0)}+\left\{k^{(H)}\sum_{l=1}^{n^{(H)}}c_l^{(H)}\hat{q}_l^{(H)}+k^{(B)}\sum_{l=1}^{n^{(B)}}c_l^{(B)}\hat{q}_l^{(B)}\right\}. \tag{5}$$

The physical idea underlying this form is that $\Delta_{HB}^{(0)}$ arises from the interaction between transition dipoles in the reference geometry, so within this dipole approximation,

$$\Delta_{HB}^{(0)}=[\mu_H\cdot\mu_B-3(\mu_H\cdot\mathbf{n}_{HB})(\mu_B\cdot\mathbf{n}_{HB})]/\epsilon R_{HB}^3, \tag{6}$$

where, μ_H, say, is the transition dipole moment vector of the H chromophore, and $\mathbf{n}_{HB}=\mathbf{R}_{HB}/R_{HB}$, with $R_{HB}=|\mathbf{R}_{HB}|$, the inter-chromophore distance in the reference geometry. The second term in Eq. (5) represents, for example, the process by which modes in the bath of chromophore B, i.e., $\{\hat{q}_l^{(B)}\}$, modify the transition dipole moment, μ_B, and effect the electronic coupling with chromophore H as the bath causes fluctuations about the reference geometry. This bath coordinate dependent inter chromophore coupling term thus provides a mechanism where by the independent baths of different chromophores can simultaneously influence a given term in the electronic Hamiltonian and thus lead to fluctuations in electronic excitation energies that are correlated to motions of the different sets of otherwise independent bath modes.

Making the usual assumptions underlying linear response theory, the properties of the system-bath interaction of interest here are determined by the relevant thermal averaged equilibrium correlation functions. For our considerations the site energy and inter-site off-diagonal coupling fluctuation correlation function terms, e.g., $C_{HH,HB}(t)=\langle\langle H|\hat{H}_{s-b}|H\rangle(t)\langle H|\hat{H}_{s-b}|B\rangle(0)\rangle$, have the forms,

$$\begin{aligned}C_{HH,HB}(t)&=\langle U^{HH}(t)U^{HB}(0)\rangle \qquad (7)\\&=k_BTk^{(H)}\sum_{l=1}^{n^{(H)}}\frac{c_l^{(H)_2}}{\omega_l^{(H)_2}}\cos\left(\omega_l^{(H)}t\right)\\&=\frac{k_BT}{\pi}k^{(H)}\int_0^\infty d\omega\frac{j^{(H)}(\omega)}{\omega}\cos(\omega t),\\C_{BB,HB}(t)&=\langle U^{BB}(t)U^{HB}(0)\rangle \qquad (8)\\&=k_BTk^{(B)}\sum_{l=1}^{n^{(B)}}\frac{c_l^{(B)_2}}{\omega_l^{(B)_2}}\cos\left(\omega_l^{(B)}t\right)\\&=\frac{k_BT}{\pi}k^{(B)}\int_0^\infty d\omega\frac{j^{(B)}(\omega)}{\omega}\cos(\omega t),\end{aligned}$$

where the angle brackets indicate thermal equilibrium ensemble averages, and here there are no cross terms in $C_{HH,HB}(t)$ or $C_{BB,HB}(t)$ related to $\langle\hat{q}^H(t)\hat{q}^B(0)\rangle$ due to the independent nature of $\hat{H}_b^H$ and $\hat{H}_b^B$. These expressions define the relevant spectral densities, $j^{(B)}(\omega)$ and $j^{(H)}(\omega)$ that, in this model, determine both the dissipation of excitation energy from the sites to their environment and how the bath mode of frequency ω correlates fluctuations in the site energies and inter-chromophore electronic couplings. These spectral densities, for example, have the following form in terms of model system-bath interaction parameters:

$$j^{(H)}(\omega)=\frac{\pi}{2}\sum_{l=1}^{n^{(H)}}\frac{c_l^{(H)_2}}{\omega_l^{(H)}}\delta\left(\omega-\omega_l^{(H)}\right). \tag{9}$$

For simplicity, with all the models considered here we assume that the spectral density that determines how the bath correlates different fluctuations has the same frequency dependence as the environmental interactions that dissipate site energy and the ks simply scale the magnitude of these interactions to give their contribution to a given correlated fluctuation. In the absence of further information about these types of frequency dependent correlations this type of model seems a reasonable first step. Calculations are currently underway to explore the appropriateness of this model for realistic applications.

The HSR two state system-bath model that provides the basis of the simplified theoretical analysis of the influence of correlations in site energy-inter-site coupling is based on more restrictive approximations. The HSR model assumes infinite temperature ($T\to\infty$) and that the correlation functions governing the system-bath interactions are infinitely rapidly decaying and makes the Markovian assumption, i.e., $C_{i,j,i',j'}(t-t')=C_{i,j,i',j'}(0)\delta(t-t')$. Despite these significant limitations, the HSR model offers some interesting predictions about how correlated fluctuations influence the coherent energy transfer in such dissipative quantum systems. According to the solution of the HSR model presented recently by Chen and Silbey,[28] the oscillation amplitude of the population and off-diagonal coherence terms in the density matrix and other dynamical properties depend predominately on the sign of the difference in the amplitudes of these site energy-inter-site electronic coupling fluctuation correlation functions, i.e., with in the Markovian approximation the zero time amplitude difference given by the quantity $[C_{HH,HB}(0)-C_{BB,HB}(0)]$ plays a central role determining many dynamical properties. Thus, for example, Chen and Silbey find that the excitation energy transfer rate involves terms such as $\sim\cos\theta\sin\theta[C_{HH,HB}(0)-C_{BB,HB}(0)]$ (Ref. 28) for their approximate analytic model. Here the mixing angle, θ, governs the transformation between the site and exciton (delocalized eigenstates of $\hat{H}_s$) representations and $\tan\theta=-2\Delta_{HB}/(\epsilon_H-\epsilon_B)$ with $(\epsilon_H-\epsilon_B)>0$. For example, their results suggest that when $\tan\theta<0$ (i.e., when $\Delta_{HB}>0$), negative values of $[C_{HH,HB}(0)-C_{BB,HB}(0)]$ will increase the amplitude of the oscillatory behavior of population and enhance the energy transfer rate, while positive values of this correlation function difference will decrease these effects.[28] To summarize if the sign of the correlation function difference $[C_{HH,HB}(0)-C_{BB,HB}(0)]$ (HH is higher energy diabat, minus BB lower energy diabat) is opposite the sign of the coupling term in the diabatic Hamiltonian, Δ_{HB}, the coherent oscillation amplitude and the energy transfer rate will both be enhanced. If the correlation function difference defined this way, and the

diabatic coupling are of the same sign these effects will be diminished.

For simplicity, here we chose $k^{(H)} = -k^{(B)}$ making $[C_{HH,HB}(0) - C_{BB,HB}(0)]$ (determined from Eq. (7)) have the largest possible positive or negative values. Physically, this corresponds to a configuration of the system in which the environmental degrees of freedom fluctuate around a reference geometry such that when the bath variables of one chromophore move they linearly increase the transition dipole of that chromophore and when the bath variables of the second chromophore move in a similar way they reduce that chromophore's transition dipole moment. This is a somewhat artificial situation that maximizes the correlation effects but, nevertheless as we will show, gives results that are indicative of general trends.

In Fig. 1, we demonstrate that the relative sign of the $k^{(H)}$ and $k^{(B)}$ can either enhance or suppress the excitation energy transfer rate, and similarly influence the magnitude and relaxation time scale of the oscillatory behavior of populations (that result from oscillations in coherence density matrix elements) in full quantum dynamics calculations that do not need to make the approximations underlying the HSR model. In the left panel of Fig. 1, for example, we see that when $[C_{HH,HB}(0) - C_{BB,HB}(0)] < 0$ ($k^{(H)} = -0.5$ and $k^{(B)} = 0.5$), the population of the initially excited H chromophore decays rapidly compared with the $k = 0$ case (i.e., the situation of independent baths coupled only to the different sites). At the same time, the oscillations of the population are also of larger amplitude compared to the $k = 0$ situation suggesting stronger long lived coherent dynamics in this case. These observations are consistent with the expectations from the HSR theory summarized above since with this model Hamiltonian $\Delta_{HB} > 0$. On the other hand, when $[C_{HH,HB}(0) - C_{BB,HB}(0)] > 0$ ($k^{(H)} = 0.5$, $k^{(B)} = -0.5$), the excitation energy transfer rate decreases and the coherent oscillatory features damp out very quickly compared to the case of independent site energy baths (i.e., the $k = 0$ case). If we choose intermediate, asymmetrical values for example, ($k^{(H)} = -0.5$ and $k^{(B)} = 0.25$) or ($k^{(H)} = 0.5$ and $k^{(B)} = 0.25$), the same sorts of trends in transfer and decoherence rates, but with somewhat less pronounced effects, are observed (not shown).

As another point of comparison, in the left panel of Fig. 1, we also explore the situation involving a separate independent off-diagonal coupling bath for which the Hamiltonian takes the form,

$$\hat{H}_{s-b}^{ind(J)} = \sum_{l=1}^{n^{(H)}} c_l^{(H)} q_l^{(H)} |H\rangle\langle H| + \sum_{l=1}^{n^{(B)}} c_l^{(B)} q_l^{(B)} |B\rangle\langle B| + \sum_{l=1}^{n^{(J)}} k c_l^{(J)} q_l^{(J)} [|H\rangle\langle B| + |B\rangle\langle H|], \tag{10}$$

where $q_l^{(J)}$ represents another set of independent harmonic bath modes that are bi-linearly coupled to the off-diagonal electronic coupling elements. To consistently determine the coupling strength of these additional independent bath oscillators to the off-diagonal inter-site electronic coupling term for this model we need to specify the off-diagonal inter-site electronic coupling-electronic coupling fluctuation correlation function, $C_{HB,HB}(t) = \langle\langle H|\hat{H}_{s-b}|B\rangle(0)\langle H|\hat{H}_{s-b}|B\rangle(t)\rangle$, which, in the independent bath case, takes the form,

$$C_{HB,HB}^{ind(J)}(t) = k_B T k^2 \sum_{l=1}^{n^{(J)}} \frac{c_l^{(J)2}}{\omega_l^{(J)2}} \cos\left(\omega_l^{(J)} t\right) = \frac{k_B T}{\pi} \int_0^\infty d\omega k^2 j^{(J)}(\omega) \frac{\cos(\omega t)}{\omega}. \tag{11}$$

Further for this independent coupling bath model we find that $C_{HH,HB}^{ind(J)}(t) = C_{BB,HB}^{ind(J)}(t) = 0$. For the correlated bath Hamiltonian in Eq. (4), on the other hand, the above electronic coupling-electronic coupling correlation function can be

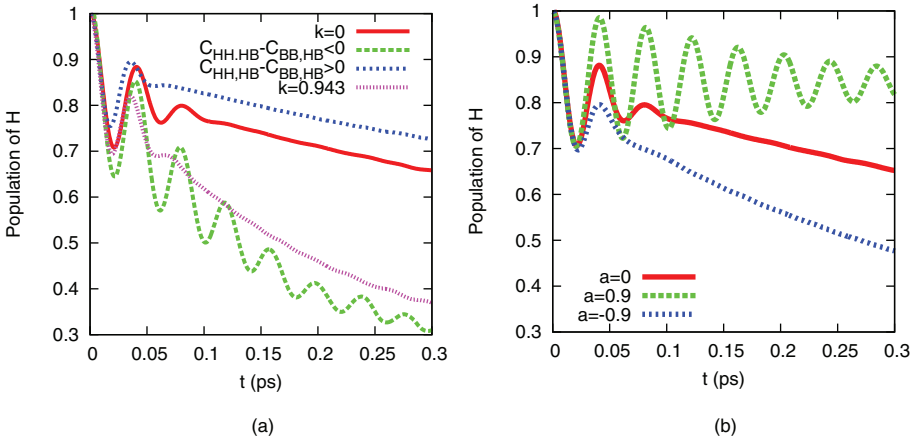

FIG. 1. Population of donor site H for model Hamiltonian including the site energy-off-diagonal coupling correlations (left panel), and site energy-site energy correlations (right panel). Various curves show results of full quantum dynamics calculations with different signs of the relevant correlation functions. The magnitude of the population oscillations can either be enhanced (for $C_{BB,HB}(0) - C_{HH,HB}(0) > 0$ (left) or $C_{HH,BB}(0) > 0$ (right)), or suppressed (if these quantities are <0). The same trends in oscillatory behavior are observed for the coherence density matrix elements ρ_{HB} (not shown). Left panel also includes results for the independent bath model that incorporates additional independent modes that are bi-linearly coupled to off-diagonal electronic Hamiltonian matrix elements that describe excitation energy transfer between sites (see text).

written as

$$C_{HB,HB}(t) = k_B T \left\{ k^{(H)2} \sum_{l=1}^{n^{(H)}} \frac{c_l^{(H)^2}}{\omega_l^{(H)^2}} \cos(\omega_l^{(B)} t) + k^{(B)^2} \sum_{l=1}^{n^{(B)}} \frac{c_l^{(B)^2}}{\omega_l^{(B)^2}} \cos\left(\omega_l^{(B)} t\right) \right\}$$
$$= \frac{k_B T}{\pi} \int_0^\infty d\omega \{ k^{(H)2} j^{(H)}(\omega) + k^{(B)2} j^{(B)}(\omega) \} \frac{\cos(\omega t)}{\omega}. \quad (12)$$

In order to make these two models have the same correlation function, $C_{HB,HB}(t)$, the following result must hold: $k^2 j^{(J)}(\omega) = k^{(H)^2} j^{(H)}(\omega) + k^{(B)^2} j^{(B)}(\omega)$. As mentioned above, for simplicity we choose the shapes of the spectral densities in all our calculations described here to be the same Debye (lorentzian) truncated form,

$$j^{(\alpha)}(\omega) = \frac{2\lambda_\alpha \omega \tau_c^{(\alpha)}}{\left[\left(\omega \tau_c^{(\alpha)}\right)^2 + 1\right]}, \quad (13)$$

with ($\alpha = H, B, \text{or} J$) and for simplicity we set $\tau_c^{(H)} = \tau_c^{(B)} = \tau_c^{(J)} = 60$ fs, but allow different solvent reorganization energies, λ_α, for the different spectral densities, in particular we choose $\lambda_H = \lambda_J = 50$ cm^{-1} and $\lambda_B = 80$ cm^{-1}, though arbitrary forms for these spectral densities can be used with the PLDM propagation approach. These values are consistent with those used in the simulations reported above. With these values and the above simplification for this independent coupling bath model we have $k = \sqrt{(k^{(H)^2}\lambda_H^2 + k^{(B)^2}\lambda_B^2)/\lambda_J^2}$ and for the parameters in the current model we find $k = 0.943$. Comparing with the results computed for this independent off-diagonal coupling model (dotted line in left panel of Fig. 1) enables us to directly explore the influence of correlated fluctuations in site energy and inter-site electronic coupling.

The agreement between the independent coupling model and the fully correlated model suggests that most of the energy transfer in the optimal case for the fully correlated model arises due to the effective correlations in off-diagonal coupling as reported by $C_{HB,HB}(t)$. The longer lived coherent oscillations apparent in the full model signal are thus associated with terms like $C_{HH,HB}(t)$, i.e., site-energy-inter-site coupling correlations do indeed prolong the observed coherent oscillations, which as mentioned above, are zero with the effective independent coupling bath model. The above results suggest that such correlations, however, are not necessary to reproduce the overall average relaxation rate but are responsible for the long lived coherent oscillations observed in the fully correlated system signals.

As one can see, the independent off-diagonal bath model of Eq. (10) gives excitation energy transfer dynamics that results in site populations that essentially decay at the same rate as observed for the correlated bath case when $k^{(H)} = -0.5$ and $k^{(B)} = 0.5$. No coherent population oscillations, however, are observed in the absence of correlation. This comparison suggests that the optimal rate of energy transfer for the fully correlated off-diagonal bath model Hamiltonian of Eq. (4) can be controlled by presence of solvent driven fluctuations in inter-site coupling and that, while correlation in site energy fluctuations and off-diagonal coupling are not critical in determining the magnitude of the overall relaxation rate, such correlations can lead to long lived oscillations in population that are the signature of coherent quantum dynamics.

As a further comparison, the result for the model of correlated fluctuations in site excitation energies ϵ_H and ϵ_B detailed in Appendix are presented in the right panel of Fig. 1. Here, both the common bath, and cross coupling bath models can be used to give the correlation between site energies, controlled by the correlation magnitude "a" (see Appendix) which can suppress or enhance coherence. From the results for this correlated site energy fluctuation model displayed in the right panel of Fig. 1 we see that increasing the positive correlation can enhance the magnitude of the population oscillations signaling long lived coherent dynamics, while decreasing the rate of energy transfer. Increasing the negative correlation, on the other hand, gives the opposite trend, i.e., an increased rate of incoherent energy transfer.

This raises the argument, if the correlation enhances the coherence, however decreases the transfer rate with the correlated site energy fluctuation model, then the primary function of the observed coherence (or correlation) cannot be enhance the efficiency in the light harvesting systems.[17] However, as we can see in the left panel of Fig. 1, as we increase the magnitude of $C_{HH,HB}(0) - C_{BB,HB}(0)$, both the magnitude of the population oscillations (i.e., quantum coherence), and the magnitude of population transfer are enhanced with the correlated inter-site coupling model. This provides a promising possible mechanism for the correlation enhancement of the excitation energy transfer rate consistent with the observation of quantum coherent beating in the experimental results.

B. Correlated fluctuations between different pairs of inter-site electronic couplings: A three state FMO model

In this section, we consider the effects of correlated fluctuations in site energy and inter-site electronic coupling between multiple pairs of coupled chromophores that share, for example, a common "bridging" chromophore. To explore these effects we require a model system with at least three coupled chromophores. To develop an understanding of the influence of correlated fluctuations in site energy and electronic couplings between states on excitation energy transfer dynamics in relevant parameter ranges we use a realistic 3 state model of the FMO photosynthetic light harvesting complex[42] where,

$$\hat{H}_s = \begin{pmatrix} \epsilon_1 & \Delta_{1,2} & \Delta_{1,3} \\ \Delta_{2,1} & \epsilon_2 & \Delta_{2,3} \\ \Delta_{3,1} & \Delta_{3,2} & \epsilon_3 \end{pmatrix} = \begin{pmatrix} 12410 & -87.7 & 5.5 \\ -87.7 & 12530 & 30.8 \\ 5.5 & 30.8 & 12210 \end{pmatrix}. \quad (14)$$

Again, the energy units here are cm^{-1}. In this model, Δ_{13} is 5–10 times smaller than the other off-diagonal electronic couplings so the system part of the Hamiltonian is approximately block diagonal and the two state theoretical analysis

of Chen and Silbey[28] can be applied separately to the different blocks. For the linearized density matrix propagation schemes we use in our calculations such simplifications are not required but with this approximation the predictions of Chen and Silbey give a good starting point for comparison. With the model Hamiltonian in Eq. (14) the mixing angle for the 12 subspace, $\tan\theta_{12} = -2\Delta_{1,2}/(\epsilon_2 - \epsilon_1)$ is positive and for the 23 subspace $\tan\theta_{23} = -2\Delta_{2,3}/(\epsilon_3 - \epsilon_2)$ is negative due to the different signs of Δ_{12} ($-87.7\ \mathrm{cm}^{-1}$) and Δ_{23} ($30.8\ \mathrm{cm}^{-1}$). Generalizing the findings above, this means that when the correlation function difference $[C_{22,12} - C_{11,12}]$ (again defined as 22 (high energy) minus 11 (low energy)) has opposite sign to Δ_{12} the coherent behavior and 12 transfer rate will be enhanced. By the same application of the Chen-Silbey solutions, since Δ_{23} is positive, the 23 subspace coherence and energy transfer rate should be enhanced if $[C_{22,12} - C_{33,12}] < 0$. A generalized multi-state implementation of the HSR theory has recently been presented and applied to a seven-state model of FMO.[29] In future work we plan to make detailed comparisons with this generalized HSR theory to test the effects of the underlying approximations and benchmark the analysis.

For the first three-state model we consider here that includes the effects of correlation in site energy and electronic coupling terms, the harmonic bath and bi-linear system-bath interaction Hamiltonian terms, $\hat{H}_b$ and $\hat{H}_{s-b}$, respectively, take the following forms:

$$\hat{H}_b = \sum_{\alpha=1}^{3}\sum_{l=1}^{n^{(\alpha)}} \frac{1}{2}\left[p_l^{(\alpha)2} + \omega_l^{(\alpha)2} q_l^{(\alpha)2}\right], \tag{15}$$

$$\begin{aligned}\hat{H}_{s-b} = &\sum_{l=1}^{n^{(1)}} c_l^{(1)} q_l^{(1)} |1\rangle\langle 1| + \sum_{l=1}^{n^{(2)}} c_l^{(2)} q_l^{(2)} |2\rangle\langle 2| \\ &+ \sum_{l=1}^{n^{(3)}} c_l^{(3)} q_l^{(3)} |3\rangle\langle 3| \\ &+ \left\{\sum_{l=1}^{n^{(1)}} k_1^{1,2} c_l^{(1)} q_l^{(1)} + \sum_{l=1}^{n^{(2)}} k_2^{1,2} c_l^{(2)} q_l^{(2)}\right\} \\ &\times [|1\rangle\langle 2| + |2\rangle\langle 1|] \\ &+ \left\{\sum_{l=1}^{n^{(2)}} k_2^{2,3} c_l^{(2)} q_l^{(2)} + \sum_{l=1}^{n^{(3)}} k_3^{2,3} c_l^{(3)} q_l^{(3)}\right\} \\ &\times [|2\rangle\langle 3| + |3\rangle\langle 2|].\end{aligned} \tag{16}$$

Here, $k_i^{i,j}$ is the rescaling coefficient that controls the strength with which the bath degrees of freedom that cause fluctuations in the energy of state $|i\rangle$ influence the electronic coupling that results in excitation transfer between states $|i\rangle$ and $|j\rangle$ through the operators $|i\rangle\langle j|$ and $|j\rangle\langle i|$. With this model Hamiltonian, bath 2 influences both the $|1\rangle\langle 2|$ and $|2\rangle\langle 3|$ electronic coupling terms thus introducing a mechanism for correlation between fluctuations in the different baths and their effects on these excitation transfer processes. The different possible non-vanishing correlation functions for this particular model are,

$$\begin{aligned}C_{12,12}(t) &= k_B T \sum_{l=1}^{n^{(1)}} \left(k_1^{1,2}\right)^2 \frac{c_l^{(1)2}}{\omega_l^{(1)2}} \cos\left(\omega_l^{(1)} t\right) \\ &\quad + \sum_{l=1}^{n^{(2)}} \left(k_2^{1,2}\right)^2 \frac{c_l^{(2)2}}{\omega_l^{(2)2}} \cos\left(\omega_l^{(2)} t\right) \\ C_{11,12}(t) &= k_B T \sum_{l=1}^{n^{(1)}} k_1^{1,2} \frac{c_l^{(1)2}}{\omega_l^{(1)2}} \cos\left(\omega_l^{(2)} t\right) \\ C_{22,12}(t) &= k_B T \sum_{l=1}^{n^{(2)}} k_2^{1,2} \frac{c_l^{(2)2}}{\omega_l^{(2)2}} \cos\left(\omega_l^{(2)} t\right) \\ C_{12,23}(t) &= k_B T \sum_{l=1}^{n^{(2)}} k_2^{1,2} k_2^{2,3} \frac{c_l^{(2)2}}{\omega_l^{(2)2}} \cos\left(\omega_l^{(2)} t\right) \\ C_{22,23}(t) &= k_B T \sum_{l=1}^{n^{(2)}} k_2^{2,3} \frac{c_l^{(2)2}}{\omega_l^{(2)2}} \cos\left(\omega_l^{(2)} t\right) \\ C_{33,23}(t) &= k_B T \sum_{l=1}^{n^{(3)}} k_3^{2,3} \frac{c_l^{(H)2}}{\omega_l^{(3)2}} \cos\left(\omega_l^{(3)} t\right) \\ C_{23,23}(t) &= k_B T \sum_{l=1}^{n^{(2)}} \left(k_2^{2,3}\right)^2 \frac{c_l^{(2)2}}{\omega_l^{(2)2}} \cos\left(\omega_l^{(2)} t\right) \\ &\quad + k_B T \sum_{l=1}^{n^{(1)}} \left(k_3^{2,3}\right)^2 \frac{c_l^{(3)2}}{\omega_l^{(3)2}} \cos\left(\omega_l^{(3)} t\right).\end{aligned} \tag{17}$$

As before, $C_{12,12}(0)$ and $C_{23,23}(0)$ are always positive and the sign of $C_{12,23}(0)$ depends on how bath 2 couple to $|1\rangle\langle 2|$ and $|2\rangle\langle 3|$. These three correlation functions, however, depend *quadratically* on the magnitude of the small correlation coupling rescaling parameters k_i^{ij}, while the site energy-inter-site coupling correlation functions, $C_{ii,ij}$ depend *linearly* on these small parameters and thus, for parameterization of the model considered in this section, are expected to play the dominant role in controlling the relaxation behavior of the system.

In the calculations summarized below the results for all the different types of correlated baths are compared with the independent model for which the system-bath Hamiltonian has the following form:

$$\begin{aligned}\hat{H}_{s-b}^{ind} = &\sum_{l=1}^{n^{(1)}} c_l^{(1)} q_l^{(1)} |1\rangle\langle 1| + \sum_{l=1}^{n^{(2)}} c_l^{(2)} q_l^{(2)} |2\rangle\langle 2| \\ &+ \sum_{l=1}^{n^{(3)}} c_l^{(3)} q_l^{(3)} |3\rangle\langle 3|.\end{aligned} \tag{18}$$

The results presented in Fig. 2 use a simplified model with the magnitude of all the different scaling coefficients $k_i^{i,j}$ set to 0.2 and we assign different signs that will influence the zero time values of the various correlation functions, which, according to the arguments presented in Sec. II A (and derived from Chen and Silbey's approximate HSR theory[28]) will

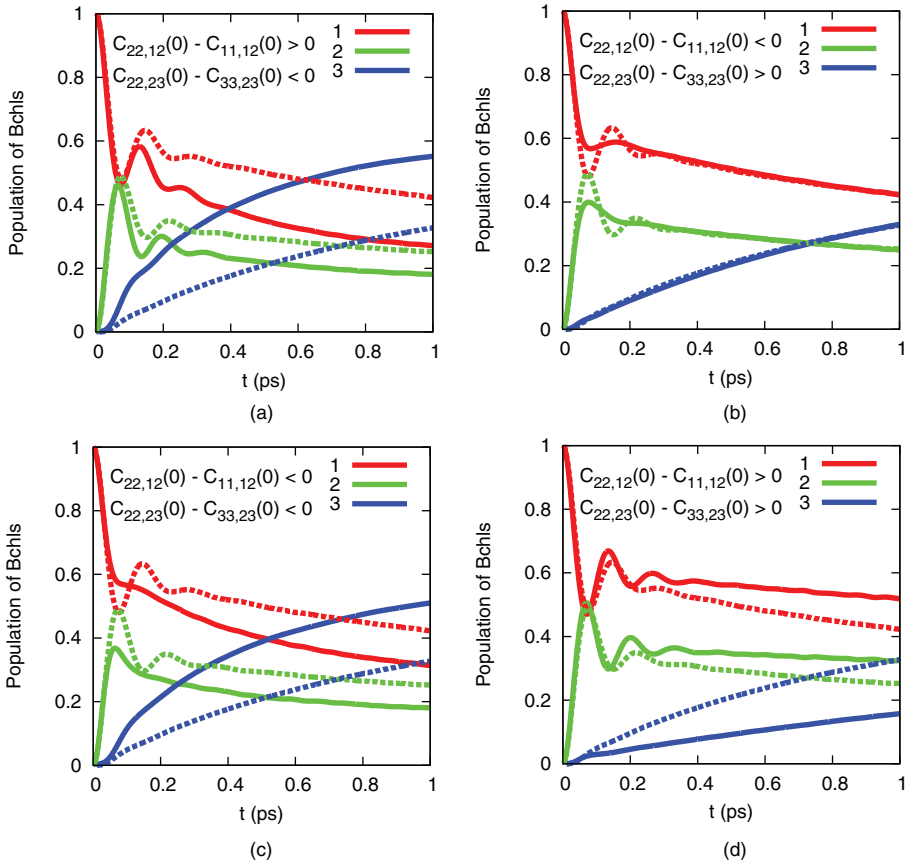

FIG. 2. Three state FMO populations for site energy-electronic coupling correlated bath model Hamiltonian in Eq. (16). Solid lines are results for the model with correlations, dashed lines give independent bath model results (Eq. (18)): (a) top left: $(k_1^{1,2}, k_2^{1,2}, k_2^{2,3}, k_3^{2,3}) = (-0.2, +0.2, -0.2, +0.2)$. (b) top right: $(k_1^{1,2}, k_2^{1,2}, k_2^{2,3}, k_3^{2,3}) = (+0.2, -0.2, +0.2, -0.2)$. (c) bottom left: $(k_1^{1,2}, k_2^{1,2}, k_2^{2,3}, k_3^{2,3}) = (+0.2, -0.2, -0.2, +0.2)$. (d) bottom right: $(k_1^{1,2}, k_2^{1,2}, k_2^{2,3}, k_3^{2,3})$ $= (-0.2,+0.2,+0.2,-0.2)$.

control the magnitude of coherent oscillations and excitation energy transfer rates between the different coupled pairs of states.

Thus in the top left panel in Fig. 2, for example, we see that when $[C_{22,12}(0) - C_{11,12}(0)] > 0$ and $[C_{22,23} - C_{33,23}(0)] < 0$, both the oscillatory features and the transfer rates are enhanced relative to the case when there are no correlations. If we change the signs so that $[C_{22,12}(0) - C_{11,12}(0)] < 0$ and $[C_{22,23}(0) - C_{33,23}(0)] > 0$ (top right of Fig. 2), we find that the oscillatory behavior quickly damps out and the population transfer rates decrease and reproduce their behavior observed in the uncorrelated model. However, if $[C_{22,12}(0) - C_{11,12}(0)] > 0$ and $[C_{22,12}(0) - C_{33,12}(0)] > 0$ (bottom right panel of Fig. 2) the coherent beating between states 1 and 2 is enhanced, but the population transfer rate to state 3 will decrease since $[C_{22,23}(0) - C_{33,23}(0)] > 0$. The bottom left panel in Fig. 2 shows the expected results for the converse situation. So the Chen-Silbey predictions based on the approximate HSR theory are robust for these conditions with the three state model in Eq. (16).

The important observation from this demonstration is that depending on the nature of correlations in the model Hamiltonian the presence of coherent beating features does not necessarily signal enhanced or diminished energy transfer. Comparing results in the top left and bottom right panels of Fig. 2, for example, we see that the population beating can be enhanced by appropriate choice of model parameters and the energy transfer can either be suppressed (bottom right) or enhanced (top left).

Next in Fig. 3, we present results for parameter sets chosen so that the various correlation function differences that play prominent roles in Chen and Silbey's two state model theory go to zero, i.e., $C_{22,12}(0) - C_{11,12}(0) = 0$ and $C_{22,23} - C_{33,23}(0) = 0$. The full Liouville matrix for the generalization of the HSR theory to three states is summarized in supplemental materials Sec. S.2.[39] Simplifying for the above model Hamiltonian and also neglecting the correlation function terms that are quadratic order in the small correlation scaling parameters, k_i^{ij} compared to the linear and zeroth order terms, the Liouville equations obtained from the matrix in supplemental materials Sec. S.2 have the following approximate form for the model considered in this section:

$$\begin{aligned}
\dot{\rho}_{11} &= i\Delta_{12}(\rho_{12} - \rho_{21}) \\
\dot{\rho}_{22} &= -i\Delta_{12}(\rho_{12} - \rho_{21}) + i\Delta_{23}(\rho_{23} - \rho_{32}) \\
\dot{\rho}_{33} &= -i\Delta_{23}(\rho_{23} - \rho_{32}) \\
\dot{\rho}_{12} &= i\Delta_{12}(\rho_{11} - \rho_{22}) + \eta_{12}\rho_{12} + \chi_{23}\rho_{13} \\
\dot{\rho}_{13} &= \chi_{23}\rho_{12} + \eta_{13}\rho_{13} + \chi_{12}^{*}\rho_{23} \\
\dot{\rho}_{23} &= i\Delta_{23}(\rho_{22} - \rho_{33}) - \eta_{23}\rho_{23} + \chi_{12}^{*}\rho_{13},
\end{aligned} \tag{19}$$

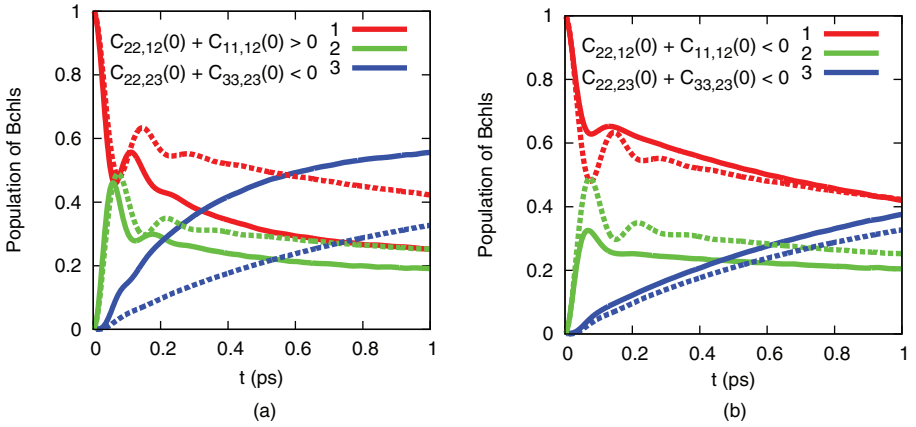

FIG. 3. Same as Fig. 2 except parameters are chosen so that now $C_{22,12} - C_{11,12} = 0$ and $C_{22,12} - C_{33,12} = 0$ and the correlation function sums have the nonzero values indicated. Again, solid lines are results for model with correlations, and dashed lines are independent bath model results. Parameters used are: (a) left: $(k_1^{1,2}, k_2^{1,2}, k_2^{2,3}, k_3^{2,3}) = (+0.2, +0.2, -0.2, -0.2)$. (b) right: $(k_1^{1,2}, k_2^{1,2}, k_2^{2,3}, k_3^{2,3}) = (-0.2, -0.2, -0.2, -0.2)$.

where $\chi_{ij} = [i\Delta_{ij} - (\gamma_{ii,ij} + \gamma_{jj,ij})]$, $\eta_{ij} = [i(\epsilon_i - \epsilon_j) - (\gamma_{ii,ii} + \gamma_{jj,jj})]$ and the other off-diagonal density matrix element equations of motion are obtained by complex conjugation. The important observation here is that the key quantities controlling the relaxation with this parameterization are correlation function sums involving the site energy-inter-site coupling fluctuation correlation functions that appear in the parameters χ_{ij}, i.e., $C_{ii,ij}(0) + C_{jj,ij}(0) = \gamma_{ii,ij} + \gamma_{jj,ij}$.

For the results presented in Fig. 3 we have chosen the $|k_i^{i,j}| = 0.2$, which means that the zero time magnitudes of the site-inter-site coupling correlations functions, $C_{ii,ij}$ are about 5 times larger than the inter-site coupling-inter-site coupling correlation functions, e.g., $C_{ij,jk}$, so ignoring these terms as in the above equations is appropriate. Under these circumstances the correlation function sum quantities, e.g., $C_{ii,ij}(0) + C_{jj,ij}(0)$, are observed in Fig. 3 to have controlling influence on the population relaxation dynamics. In the right panel of Fig. 3, for example, we see that having both correlation function sums negative has little influence on the population relaxation dynamics though it does cause more rapid damping of the coherent population oscillation compared to the uncorrelated situation. Making the sign of $[C_{22,12}(0) + C_{11,12}(0)] > 0$ but keeping $[C_{22,23}(0) + C_{22,23}(0)] < 0$ is seen to enhance the rate of energy transfer from state 1 to state 3, leaving the state 2 population dynamics essentially unchanged. Note the Hamiltonian for this model is constructed so that the direct coupling between states 1 and 3 is small and so the energy must be transferred through the intermediate state 2. Generally for this type of model we see that initial state 1 and intermediate state 2 show short time coherent oscillation of their populations. The terminal state 3, which is fed by coupling to intermediate state 2, on the other hand, shows essentially no remnant of the initial coherence between the 1 and 2 dimer system and we observe incoherent exponential growth in the population of terminal state 3.

The final class of model Hamiltonians that we consider in this paper has, in addition to the baths describing the independent relaxation of the three sites, further groups of independent bath oscillators that interact with the inter-site electronic coupling terms to include correlation in the fluctuations of these couplings. The first such model we consider includes a set of bath oscillators that interact with the inter-site electronic coupling terms in such a way as to account for correlation in the fluctuations of coupling between sites 1–2 and sites 2–3. The various terms included in this model Hamiltonian are thus detailed in equations below:

$$\hat{H}_b = \sum_{\alpha=1}^{3}\sum_{l=1}^{n^{(\alpha)}} \frac{1}{2}\left[p_l^{(\alpha 2)} + \omega_l^{(\alpha 2)} q_l^{(\alpha 2)}\right] + \sum_{l=1}^{n^{(123)}} \frac{1}{2}\left[p_l^{(123)2} + \omega_l^{(123)2} q_l^{(123)2}\right], \tag{20}$$

$$\begin{aligned}\hat{H}_{s-b} = &\sum_{l=1}^{n^{(1)}} c_l^{(1)} q_l^{(1)} |1\rangle\langle 1| + \sum_{l=1}^{n^{(2)}} c_l^{(2)} q_l^{(2)} |2\rangle\langle 2| \\ &+ \sum_{l=1}^{n^{(3)}} c_l^{(3)} q_l^{(3)} |3\rangle\langle 3| \\ &+ \sum_{l=1}^{n^{(123)}} k_{123}^{1,2} c_l^{(123)} q_l^{(123)} [|1\rangle\langle 2| + |2\rangle\langle 1|] \\ &+ \sum_{l=1}^{n^{(123)}} k_{123}^{2,3} c_l^{(123)} q_l^{(123)} [|2\rangle\langle 3| + |3\rangle\langle 2|],\end{aligned} \tag{21}$$

and the fluctuations in the inter-site coupling-inter-site coupling terms in this model are described by the correlation functions,

$$\begin{aligned}C_{12,12}(t) &= k_B T \sum_{l=1}^{n^{(123)}} \left(k_{123}^{1,2}\right)^2 \frac{c_l^{(123)2}}{\omega_l^{(123)2}} \cos\left(\omega_l^{(123)} t\right) \\ C_{12,23}(t) &= k_B T \sum_{l=1}^{n^{(123)}} k_{123}^{1,2} k_{123}^{2,3} \frac{c_l^{(123)2}}{\omega_l^{(123)2}} \cos\left(\omega_l^{(123)} t\right) \\ C_{23,23}(t) &= k_B T \sum_{l=1}^{n^{(123)}} \left(k_{123}^{2,3}\right)^2 \frac{c_l^{(123)2}}{\omega_l^{(123)2}} \cos\left(\omega_l^{(123)} t\right).\end{aligned} \tag{22}$$

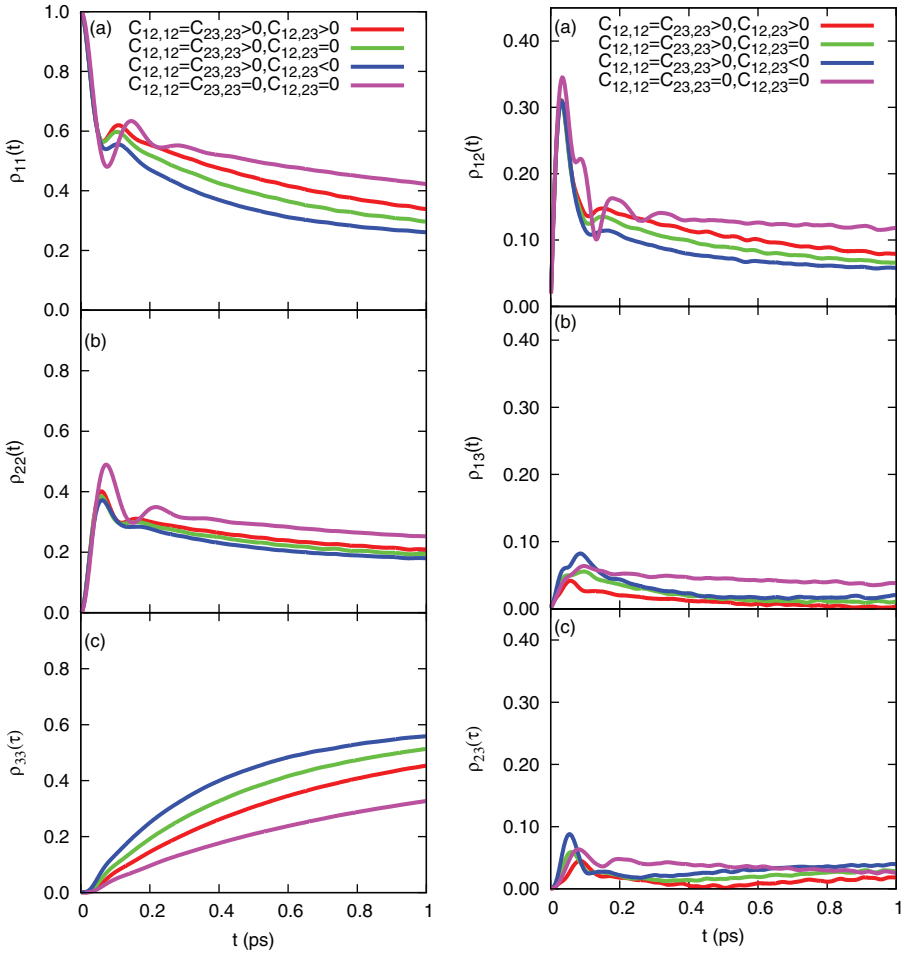

FIG. 4. Comparison of density matrix dynamics results for various models that include correlated fluctuations in electronic coupling between chromophores. Left panel shows state populations, while right panel displays off-diagonal or coherence density matrix elements computed in the site basis. The magenta curves give results computed for the original independent bath model, the green curves are computed using the model Hamiltonian with two independent electronic coupling baths in Eq. (24). The red and blue curves are computed with the common coupling bath model determined by the Hamiltonian in Eq. (21). In this case the magnitudes of the rescaling factors (the ks in these equations) are 0.4, and the signs are chosen to give the indicated signs of the correlation functions, e.g., $C_{12,23}$, etc.

For comparison, in the final model we consider here, we remove the terms that correlate fluctuations in coupling between the two dimers, and incorporate independent baths describing uncorrelated fluctuations in the independent dimer couplings. Thus, this final model is described by the following Hamiltonian terms:

$$\hat{H}_b = \sum_{\alpha=1}^{3}\sum_{l=1}^{n^{(\alpha)}} \frac{1}{2}\left[p_l^{(\alpha)2} + \omega_l^{(\alpha)2} q_l^{(\alpha)2}\right] \tag{23}$$

$$+ \sum_{l=1}^{n^{(12)}} \frac{1}{2}\left[p_l^{(12)2} + \omega_l^{(12)2} q_l^{(12)2}\right]$$

$$+ \sum_{l=1}^{n^{(23)}} \frac{1}{2}\left[p_l^{(23)2} + \omega_l^{(23)2} q_l^{(23)2}\right],$$

$$\hat{H}_{s-b} = \sum_{l=1}^{n^{(1)}} c_l^{(1)} q_l^{(1)} |1\rangle\langle 1| + \sum_{l=1}^{n^{(2)}} c_l^{(2)} q_l^{(2)} |2\rangle\langle 2| \tag{24}$$

$$+ \sum_{l=1}^{n^{(3)}} c_l^{(3)} q_l^{(3)} |3\rangle\langle 3|$$

$$+ \sum_{l=1}^{n^{(12)}} k^{1,2} c_l^{(12)} q_l^{(12)} [|1\rangle\langle 2| + |2\rangle\langle 1|]$$

$$+ \sum_{l=1}^{n^{(23)}} k^{2,3} c_l^{(23)} q_l^{(23)} [|2\rangle\langle 3| + |3\rangle\langle 2|],$$

and the non-vanishing inter-site coupling correlation functions for this model are,

$$C_{12,12}(t) = k_B T \sum_{l=1}^{n^{(12)}} (k^{1,2})^2 \frac{c_l^{(12)2}}{\omega_l^{(12)2}} \cos(\omega_l^{(12)} t) \tag{25}$$

$$C_{23,23}(t) = k_B T \sum_{l=1}^{n^{(23)}} (k^{2,3})^2 \frac{c_l^{(23)2}}{\omega_l^{(23)2}} \cos(\omega_l^{(23)} t).$$

For these last two models, because the relevant correlation functions depend only quadratically on the bath interaction correlation rescaling parameters (the ks) we have set their magnitudes to be $|k| = 0.4$ so $k^2 \sim 0.2$, which makes these terms in this model of comparable magnitude to the dominant linear terms in the previous model that incorporated site

energy-inter-site coupling correlations (whose magnitude we set by choosing $|k| = 0.2$ for these earlier models).

The evolution of the populations and coherence density matrix elements for the models outlined above are compared in Fig. 4. The results presented here show that in the absence of correlation in inter-site electronic coupling fluctuations (magenta curves) oscillations in the ρ_{12} coherence persist out to about 400 fs (the bare model was fit to reproduce this experimental observation) and in this situation the energy transfer rate as measured by the growth in population, ρ_{33}, is slowest. Adding correlated inter-site coupling fluctuations so that $C_{12,12} = C_{23,23} > 0$ (red, green, and blue curves) generally increases the energy transfer rate, but also damps out the oscillations in coherence more rapidly. The overall magnitude of the increase in energy transfer rate is observed to depend on the strength and sign of the inter-dimer coupling fluctuation correlation function, $C_{12,23}$, with the largest increase in energy transfer rate occurring when $C_{12,23} < 0$, and in this case the transfer rate is nearly double that of when there are no correlations in inter-site couplings.

From Fig. 4 we see that in all cases including fluctuations in the electronic coupling matrix elements, whether they involve correlation, or not, increase the energy transfer rate and reduce the coherence time. In order to recover the experimentally observed long lived coherence relaxation time scale with a model that includes environment induced fluctuations in electronic coupling, the magnitude of the electronic coupling in the bare model system Hamiltonian (e.g., the $\Delta^{(0)}_{i,j}$ in Eq. (5)) would need to be increased. Interestingly, the coherence relaxation time observed with the different treatments of correlated fluctuations in Fig. 4 seem to be largely independent of the nature of the correlation.

III. CONCLUSIONS

In this paper, we have employed accurate semiclassical quantum dynamics methods that can reliably treat general models for dissipative open quantum system-bath dynamics to explore the characteristics of excitation energy transfer processes in a number of general paradigms for incorporating the effects of various types of correlated fluctuations in model system parameters driven by interactions with the environment. While the calculations we report here have been focused on models for excitation energy transfer in photosynthetic light harvesting systems, due to the availability of highly detailed recent nonlinear optical spectroscopy studies on these systems that report the timescales for the competition between coherent and incoherent dynamics in these processes, our approach should be generally applicable to study models for similar quantum processes that may play important roles in, for example, electron transport in nanostructured complex systems where donors and acceptors (of either excitation energy or electrons) are embedded with sufficient density, in an environment capable of fluctuating on a range of length-scales including those characteristic of the inter donor-acceptor interactions that are responsible for the transport processes of interest.

While the models we have studied here have been of a fairly standard multi-state system-bi-linearly coupled harmonic bath form, the semi-classical quantum dynamics methods that we have developed, and employed for these studies are generally applicable to more complex models and do not require the use of Markovian, secular or high temperature approximations, or even the use of perturbation theory. As such the general findings of our studies provide an important benchmark for testing approximate approaches to understanding the effects of correlated fluctuations on dissipative quantum dynamics in complex systems.

To summarize the findings of these studies, our main focus here has been on building model Hamiltonians that can capture how environmental modes might modulate, in a correlated way, the *off-diagonal* couplings between electronic states in which excitation energy is localized at different interacting sites. Appendix presents some results obtained for more standard models[7–9,22,26] that incorporate correlated fluctuations in *diagonal* site excitation energies. For these models we generally find that as the strength of correlation is increased, the quantum coherent oscillation in populations can be enhanced, but with such models, in this strongly correlated regime, the energy transfer rate will be slowed down significantly. Thus *enhanced coherent dynamics* with correlated site energy fluctuations causes *slower* energy transfer with these sorts of models. In contrast, in the main body of the paper we show that with more general model Hamiltonians that incorporate the effects of correlated fluctuations in the *off-diagonal* electronic couplings (as well as in the diagonal site energies) the range of energy transport behaviors that can be addressed are much more varied and interesting. Thus, for example, the relative sign and strength of different types of correlations can be adjusted to give situations in which we simultaneously enhance the population beating signatures of quantum coherence *and* increase the energy transfer rate between donor and acceptor sites whose off-diagonal electronic couplings are correlated appropriately by environmental fluctuations. In fact, a wide range of possibilities open up with model Hamiltonians with this type of flexibility.

Several theoretical groups[11–15] have begun exploring detailed microscopic simulation models looking for different types of environment driven correlated fluctuations in chromophore electronic properties. The ubiquitous finding from the various photosynthetic energy transfer systems studied so far is that fluctuations in site energies seem to be such that on average they are *uncorrelated*. However, there is evidence that the fluctuations in electronic couplings between different pairs of chromophores show correlation. It thus seems unlikely that the situation in real systems is as restrictive as the simple correlated site energy fluctuation model would suggest and more work both from the experimental and theoretical directions to elucidate the nature of such correlations and their influence on dynamics needs to be done with the aim to begin to design environments that can be self-assembled to take advantage of these correlations as a mechanism to control energy and charge transport in fluctuating nano-structured environments. Powerful new approaches, like quantum process tomography,[52] are in principle capable of combining advanced multidimensional electronic spectroscopies with quantum dynamical theoretical methods to enable extraction of the detailed quantum information necessary

to build more realistic models that can accurately parameterize the more general classes of models for correlated fluctuations that we have begun exploring in this paper.

ACKNOWLEDGMENTS

We would like to dedicate this publication to the memory of Bob Silbey. He, and his work in this area, will continue to be an inspiration to us, and indeed the whole field. We gratefully acknowledge support for this research from the National Science Foundation (NSF) under Grant No. CHE-0911635. D.F.C. acknowledges the support of his Stokes Professorship in Nanobiophysics and Principle Investigator Grant No. 10/IN.1 / I3033 from Science Foundation Ireland. P.H. appreciates discussions with Sara Bonella and Xin Chen. We also acknowledge a grant of supercomputer time from the Boston University Office of Information Technology and Scientific Computing and Visualization.

APPENDIX A: QUANTUM DYNAMICS OF CORRELATED SITE ENERGY FLUCTUATION MODELS

In this appendix, we present the results of our quantum dynamics calculations on the model that was fit to reproduce the experimental data on excitation energy transfer between the accessory bacteriochlorophyll (Bchl or B) and bacteriopheophytin (BPhy or H) chromophores embedded in the transmembrane protein scaffolding near the reaction center of *Rhodobacter sphaeroides* as reported by Lee *et al.*[1] To fit the experimental spectral dynamics reasonably, these authors found that they could assume the fluctuations in the B and H site energies were strongly correlated, giving rise to in-phase energy fluctuations that preserved coherence.[1] It was found that strong electronic coupling, which could also lead to longer lived coherence, would not give a reasonable fit to experimental data.[1] These authors did not consider the generalized model that allows for inter-site coupling-inter-site coupling correlations explored in the present work.

The total Hamiltonian for this experimentally fitted model based on correlated site energy fluctuations is described by four terms,

$$\hat{H} = \hat{H}_s + \hat{H}_{s-b} + \hat{H}_b + \hat{H}_{brown} \tag{A1}$$

Here the two state electronic subsystem part of the Hamiltonian is given in Eq. (2), and $\hat{H}_b$ and $\hat{H}_{s-b}$ are the bath and system-bath interaction terms, respectively. The term $\hat{H}_{brown}$ describes the vibrations of a damped protein mode (a Brownian oscillator) that was observed to modulate the experimental signals. The detailed treatment of this Brownian mode will be outlined later. In the calculations outlined here we have considered two different models for the bath and system-bath interaction terms based on different descriptions for how environmental effects might cause correlation in site energy fluctuations.

First, the ***common bath model***[9,24] assumes that chromophores H and B have their own harmonic baths, and we also introduce a set of modes that are "common" to both chromophores so the common bath model Hamiltonian has the form,

$$\begin{aligned}\hat{H}_b^{com} &= \sum_{\alpha=H,B}\sum_{l=1}^{n^{(\alpha)}}\frac{1}{2}\left[p_l^{(\alpha)2}+\omega_l^{(\alpha)2}q_l^{(\alpha)2}\right] \\ &\quad+\sum_{m=1}^{n_{com}^{(HB)}}\frac{1}{2}\left[P_m^{(HB)2}+\Omega_m^{(H,B)2}Q_m^{(HB)2}\right] \\ \hat{H}_{s-b}^{com} &= \left[\sum_{l=1}^{n^{(H)}}\tilde{c}_l^{(H)}q_l^{(H)}+\sum_{m=1}^{n_{com}^{(HB)}}\tilde{C}_m^{(H)}Q_m^{(HB)}\right]|H\rangle\langle H| \\ &\quad+\left[\sum_{l=1}^{n^{(B)}}\tilde{c}_l^{(B)}q_l^{(B)}+\sum_{m=1}^{n_{com}^{(HB)}}\tilde{C}_m^{(B)}Q_m^{(HB)}\right]|B\rangle\langle B|.\end{aligned} \tag{A2}$$

The second bath model is the so-called ***cross coupling model***[23] that again includes different bath modes for the H and B chromophores. With the cross coupling model, however, there are coefficients x_{BH}, for example, that scale the strength of coupling of the H bath modes to the B chromophore and *visa versa*, so the bath Hamiltonian terms for this cross coupling model have the following form:

$$\begin{aligned}\hat{H}_b^{cross} &= \sum_{\alpha=H,B}\sum_{l=1}^{n^{(\alpha)}}\frac{1}{2}\left[p_l^{(\alpha)2}+\omega_l^{(\alpha)2}q_l^{(\alpha)2}\right] \\ \hat{H}_{s-b}^{cross} &= \left\{x_{HH}\sum_{l=1}^{n^{(H)}}c_l^{(H)}q_l^{(H)}\right. \\ &\quad\left.+x_{HB}\sum_{l=1}^{n^{(B)}}c_l^{(B)}q_l^{(B)}\right\}|H\rangle\langle H| \\ &\quad+\left\{x_{BH}\sum_{l=1}^{n^{(H)}}c_l^{(H)}q_l^{(H)}\right. \\ &\quad\left.+x_{BB}\sum_{l=1}^{n^{(B)}}c_l^{(B)}q_l^{(B)}\right\}|B\rangle\langle B|,\end{aligned} \tag{A3}$$

In the common bath model $q_l^{(H)}$, $q_l^{(B)}$ represent the lth independent bath oscillator that couple to the $|H\rangle$ or $|B\rangle$ states, respectively, with coupling strengths $\tilde{c}_l^{(H)}$ and $\tilde{c}_l^{(B)}$. The mth common bath oscillator mode $Q_m^{(HB)}$ couples to both the $|H\rangle$ and $|B\rangle$ states simultaneously. With this model, these common bath modes give rise to correlated energy level fluctuations when the common bath coupling constants $\tilde{C}_m^{(H)}$ and $\tilde{C}_m^{(B)}$ are not zero.

In the cross coupling model, the correlation is introduced by making the energy of a given chromophore depend both on its own bath coordinates and on the bath coordinates associated with another chromophore's bath. In this model, for example, $q_l^{(B)}$ is the lth mode that would normally be independently coupled to chromophore B with coupling strength $c_l^{(B)}$. With the cross coupling model, however, by introducing the cross coupling, this mode is also coupled to chromophore state $|H\rangle$ with rescaled cross correlation factor x_{HB}.

The approach employed in fitting the experimental data[1] assumes a model for the correlated fluctuations in site

excitation energies of the B and H chromophores based on the strength of correlation, a, specified by the following relationship between the different spectral densities

$$j^{(HB)}(\omega) = |a|\sqrt{j_{tot}^{(H)} j_{tot}^{(B)}(\omega)}, \tag{A4}$$

where the spectral densities, for example, $j_{tot}^{(H)}(\omega)$ and $j^{(HB)}(\omega)$ determine the site energy correlation function, $C_{HH,HH}(t)$, and cross-correlation function, $C_{HH,BB}(t)$, respectively. The value of the correlation strength defined in this way obtained from the fit to experimental data[1] is $a = 0.9$.

In order to connect this assumed relationship between spectral densities and the model Hamiltonians outlined above, our analysis starts by using the models to compute these various correlation functions defined as follows: $C_{HH,BB}(t) = \langle\langle H|\hat{H}_{s-b}(t)|H\rangle\langle B|\hat{H}_{s-b}(0)|B\rangle\rangle = \langle U_{HH}(t)U_{BB}(0)\rangle$, the cross-correlation function correlates fluctuations in site energies of the different chromophores, and $C_{HH,HH}(t) = \langle U_{HH}(t)U_{HH}(0)\rangle$, is the regular site excitation energy fluctuation correlation function. The Hamiltonians for the different bi-linear system-harmonic bath interaction models given above can be used to compute exact expressions for these various correlation functions written in terms of the spectral densities. The relationship in Eq. (A4) is thus used to give a consistent specification of the model Hamiltonian parameters.

For the common bath model, for example, the site excitation energy fluctuation correlation function, e.g., $C_{HH,HH}(t)$, will be determined by the total spectral density, $j_{tot}^{(H)}$, arising from all influences of the protein environment on chromophore H. From Eq. (A2) $j_{tot}^{(H)}$ contains contributions from both the independent bath modes of this chromophore, $q_l^{(H)}$, and from the common bath modes, $Q_m^{(HB)}$. The general relationship between the spectral density and the correlation function is: $C_{HH,HH}(t) = \frac{\hbar}{\pi}\int_0^\infty d\omega j_{tot}^{(H)}(\omega)[\coth(\hbar\beta\omega/2)\cos(\omega t) - i\sin(\omega t)]$.

In Ref. 1 a simple ohmic with Lorentzian truncation form, $j_{tot}^{(\alpha)}(\omega) = 2\lambda^{(\alpha)}(\omega\tau_c{}^{\alpha})/[(\omega\tau_c{}^{\alpha})^2 + 1]$, (with α = H or B) is assumed for this total spectral density, and the following values of reorganization energy and relaxation time: $\lambda^H = 50\ \text{cm}^{-1}$ and $\lambda^B = 80\ \text{cm}^{-1}$, $\tau_c{}^H = \tau_c{}^B = 60$ fs, are used. This model also incorporates static disorder for each of the site energies with $\delta^H = \delta^B = 20\ \text{cm}^{-1}$, however, for simplicity we neglect the contribution of static disorder in the cross-correlation function as it has only a minor effect on the dynamics for this system. Thus, in the limit where $\hbar \to 0$, this experimentally determined total spectral density for the common bath model can be related through the following classical result to the site energy fluctuation correlation function:[53]

$$\begin{aligned} C_{HH,HH}^{com}(t) &= \frac{k_BT}{\pi}\int_0^\infty d\omega \frac{j_{tot}^{(H)}(\omega)}{\omega}\cos(\omega t) \\ &= k_BT\sum_{l=1}^{n^{(H)}}\frac{\tilde{c}_l^{(H)2}}{\omega_l^{(H)2}}\cos\left(\omega_l^{(H)}t\right) \\ &\quad + k_BT\sum_{m=1}^{n_{com}^{(HB)}}\frac{\tilde{C}_m^{(H)2}}{\Omega_m^{(HB)2}}\cos\left(\Omega_m^{(HB)}t\right) \\ &= \frac{k_BT}{\pi}\int_0^\infty d\omega \frac{j_{ind}^{(H)}(\omega)}{\omega}\cos(\omega t) \\ &\quad + \frac{k_BT}{\pi}\int_0^\infty d\omega \frac{j_{com}^{(H)}(\omega)}{\omega}\cos(\omega t), \end{aligned} \tag{A5}$$

with similar structure of $C_{BB,BB}^{com}(t)$, and here we have defined the component, "independent" and "common" bath spectral densities as, respectively: $j_{ind}^{(H)}(\omega) = \frac{\pi}{2}\sum_{l=1}^{n^{(H)}}(\tilde{c}_l^{(H)2}/\omega_l^{(H)})\delta(\omega - \omega_l^{(H)})$ and $j_{com}^{(H)}(\omega) = \frac{\pi}{2}\sum_{m=1}^{n_{com}^{(HB)}}(\tilde{C}_m^{(H)2}/\Omega_m^{(HB)})\delta(\omega - \Omega_m^{(HB)})$. From the above result, for this common bath model, we find that

$$j_{tot}^{(H)}(\omega) = j_{ind}^{(H)}(\omega) + j_{com}^{(H)}(\omega), \tag{A6}$$

and with these definitions $j_{ind}^{(H)}(\omega)$, $j_{com}^{(H)}(\omega)$, and $j_{tot}^{(H)}(\omega)$ are all positive definite. The single parameter relationship underlying the fitting form assumed in Eq. (A4) can be related to the common bath model parameterization by identifying the correlation strength (absolute value of a) as the fraction of the total spectral density represented by the common bath component, i.e., $|a| = j_{com}^{(H)}(\omega)/j_{tot}^{(H)}(\omega)$ and, dividing the above result by $j_{tot}^{(H)}(\omega)$, gives $1 - |a| = j_{ind}^{(H)}(\omega)/j_{tot}^{(H)}(\omega)$. So with this simplest of interpretations the spectral densities all have the same frequency dependence (shape) as $j_{tot}^{(H)}(\omega)$ but their relative strengths are scaled by $|a|$, thus for example $j_{com}^{(H)}(\omega) = |a|j_{tot}^{(H)}(\omega)$, etc. The model underlying Eq. (A4) supposes that the same scaling factor, a, also relates the various spectral densities of the bath of chromophore B to its total spectral density, so e.g., $j_{com}^{(B)}(\omega) = |a|j_{tot}^{(B)}(\omega)$.

Also due to the introduction of the common coupling modes in the common bath model, the cross-correlation function $C_{HH,BB}^{com}(t)$ is non-zero and has the form,

$$\begin{aligned} C_{HH,BB}^{com} &= \frac{k_BT}{\pi}\int_0^\infty d\omega \frac{j_{com}^{(HB)}(\omega)}{\omega}\cos(\omega t) \\ &= k_BT\sum_{m=1}^{n_{com}^{(HB)}}\frac{\tilde{C}_m^{(H)}\tilde{C}_m^{(B)}}{\Omega_m^{(HB)2}}\cos\left(\Omega_m^{(HB)}t\right), \end{aligned} \tag{A7}$$

where we have defined the common bath spectral density as

$$j_{com}^{(HB)}(\omega) = \frac{\pi}{2}\sum_{m=1}^{n_{com}^{(HB)}}\left(\tilde{C}_m^{(H)}\tilde{C}_m^{(B)}/\Omega_m^{(HB)}\right)\delta\left(\omega - \Omega_m^{(HB)}\right), \tag{A8}$$

which, depending on the relative signs of the system-common bath coupling constants $\tilde{C}_m^{(H)}$ and $\tilde{C}_m^{(B)}$ could either be positive (correlated common bath for H and B) or negative (anti-correlated).

Finally, from the definitions in Eqs. (A5) and (A7), the heights of each δ-distribution at a given common bath mode frequency require that the common bath spectral densities satisfy the following equality $(j_{com}^{(HB)}(\omega))^2 = j_{com}^{(H)}(\omega)j_{com}^{(B)}(\omega)$. Substituting the expressions obtained above, i.e., $j_{com}^{(H)}(\omega) = |a|j_{tot}^{(H)}(\omega)$, and $j_{com}^{(B)}(\omega) = |a|j_{tot}^{(B)}(\omega)$ we arrive at the assumed spectral density relationship within the common bath model Hamiltonian formulation: $j_{com}^{(HB)}(\omega) = |a|\sqrt{j_{tot}^{(H)}(\omega)j_{tot}^{(B)}(\omega)}$, giving a useful physical interpretation for the strength of correlation $|a|$.

For cross coupling model, these correlation functions can be expressed as

$$\begin{aligned} C^{cross}_{HH,HH}(t) &= \frac{k_B T}{\pi}\int_0^\infty d\omega \frac{\cos(\omega t)}{\omega}\left[x^2_{HH} j^{(H)}_{tot}(\omega) + x^2_{HB} j^{(B)}_{tot}(\omega)\right] \\ &= k_B T\left[\sum_{l=1}^{n^{(H)}} x^2_{HH}\frac{c^{(H)2}_l}{\omega^{(H)2}_l}\cos(\omega^{(H)}_l t) + \sum_{l=1}^{n^{(B)}} x^2_{HB}\frac{c^{(B)2}_l}{\omega^{(B)2}_l}\cos\left(\omega^{(B)}_l t\right)\right] \\ C^{cross}_{HH,BB}(t) &= \frac{k_B T}{\pi}\int_0^\infty d\omega \frac{\cos(\omega t)}{\omega}\left[x_{HH}x_{BH} j^{(H)}_{tot}(\omega) + x_{HB}x^2_{BB} j^{(B)}_{tot}(\omega)\right] \\ &= k_B T\left[\sum_{l=1}^{n^{(H)}} x_{HH}x_{BH}\frac{c^{(H)2}_l}{\omega^{(H)2}_l}\cos(\omega^{(H)}_l t) + \sum_{l=1}^{n^{(B)}} x_{HB}x_{BB}\frac{c^{(B)2}_l}{\omega^{(B)2}_l}\cos(\omega^{(B)}_l t)\right]. \end{aligned} \tag{A9}$$

These expressions can be rewritten using short hand definitions of C_{HH} and C_{HB}, giving the following system of equations: $C_{HH} = x^2_{HH}C_{HH} + x^2_{HB}C_{BB}$, $C_{BB} = x^2_{BH}C_{HH} + x^2_{BB}C_{BB}$, $C_{HB} = x_{HH}x_{BH}C_{HH} + x_{HB}x_{BB}C_{BB}$, $C_{BH} = x_{BH}x_{HH}C_{HH} + x_{BB}x_{HB}C_{BB}$. Writing each correlation function in terms of the total spectral densities and substituting the Lorentzian truncated ohmic forms with the appropriate combination of reorganization energies, λ_K obtained using Eq. (A4), we obtain: $\lambda^H = x^2_{HH}\lambda^H + x^2_{HB}\lambda^B$, $\lambda^B = x^2_{BH}\lambda^H + x^2_{BB}\lambda^B$, $a\sqrt{\lambda^H\lambda^B} = x_{HH}x_{BH}\lambda^H + x_{HB}x_{BB}\lambda^B$, $a\sqrt{\lambda^B\lambda^H} = x_{BH}x_{HH}\lambda^H + x_{BB}x_{HB}\lambda^B$, and the solution is[23]

$$\begin{pmatrix} x_{HH} & x_{HB} \\ x_{BH} & x_{BB} \end{pmatrix} = \frac{1}{\sqrt{1+\zeta^2}}\begin{pmatrix} 1 & \left(\frac{\lambda_H}{\lambda_B}\right)^{1/2}\zeta \\ \left(\frac{\lambda_B}{\lambda_H}\right)^{1/2}\zeta & 1 \end{pmatrix}, \tag{A10}$$

where $a = \frac{2\zeta}{1+\zeta^2}$. We can see that although $C_{HB} = C_{BH}$ is required, it is not necessary for $x_{BH} = x_{HB}$, which means the **x** matrix could be non-Hermitian.

The calculation results reported below with these different models have $T = 180$ K. We find that the common bath model and cross coupling model for this two state system give identical descriptions of the exciton dynamics due to the equivalence of the correlation functions with these models.

As mentioned earlier, the model Hamiltonian in Eq. (A1) developed by Lee *et al.*[1] includes an explicit additional mode that modulates the excitation energy of the H state so as to capture the low frequency oscillation observed in the experimental signal. The behavior of the signal suggests that this mode exhibits damped oscillatory motion and so it is modeled as a Brownian mode, Q_b, with frequency, Ω_b, that couples to the population of state $|H\rangle$ with bi-linear coupling strength C_b, as well as to its own dissipative bath of harmonic oscillators with coordinates $q^{(b)}_i$. Thus this Brownian oscillator term, $\hat{H}_{brown}$, in Eq. (A1) has the following form:

$$\begin{aligned} \hat{H}_{brown} &= \frac{1}{2}\left[P_b^2 + \Omega_b^2 Q_b^2\right] + C_b Q_b |H\rangle\langle H| \\ &+ \sum_{i=1}^{n_b}\left\{\frac{1}{2}\left[p^{(b)2}_i + \omega^{(b)2}_i q^{(b)2}_i\right] + \left[c^{(b)}_i q^{(b)}_i Q_b + \frac{c^{(b)2}_i Q_b^2}{2\omega^{(b)2}_i}\right]|H\rangle\langle H|\right\}. \end{aligned} \tag{A11}$$

The physical origin of this mode is a low frequency collective protein vibration. Here $C_b = \sqrt{2\Omega_b S}\Omega_b$ (with $\hbar = 1$), $\Omega_b = 250$ cm^{-1} is the frequency of the Brownian vibrational mode and $S = 0.4$ is the Huang-Rhys factor. The coupling strength, $c^{(b)}_i$, between the dissipative bath mode q_i and the Brownian mode, is sampled from the spectral density: $j_b(\omega) = \gamma\omega\exp^{-\omega/\Lambda}$, where the γ=50 cm^{-1} is the damping constant of the bath for the Brownian mode and $\Lambda = 100$ cm^{-1} is the cutoff frequency for this dissipative bath.

In the calculations, we explored three different initial conditions for the Brownian mode: (1) The trajectories have an initial phase shift $\phi = 0.28$, which means that the initial condition has either Q_b sampled from $Tr_{P_b}\rho_w \sim \tanh(\beta\Omega_b/2)e^{-\left[\tanh(\beta\Omega_b/2)\Omega_b\right]\left[(\Omega_b^2 Q_b^2/2)\right]}$, i.e., the momentum integrated Wigner density, and $P_b = \tan\phi Q_b$ or; (2) $Q_b = \sqrt{\frac{1}{\Omega_b}}\cos\phi$ and $P_b = \sqrt{\Omega_b}\sin\phi$, or finally; (3) the thermal distribution (Wigner density), $\rho_w = \tanh(\beta\Omega_b/2)e^{-\left[\tanh(\beta\Omega_b 2)/\Omega_b\right]\left[P_b^2/2+(\Omega_b^2 Q_b^2/2)\right]}$ was used to sample both Q_b and P_b. With this thermal sampling we average over a uniform relative phase distribution.

According to Garg *et al.*,[44] this Brownian model can be expressed as an equivalent system-bath model, $\hat{H}^{trans}_{brown}$, through a coordinate transformation giving,

$$\hat{H}^{trans}_{brown} = \sum_{i=1}^{\tilde{n}}\left\{\frac{1}{2}\left[\tilde{p}^{(b)2}_i + \tilde{\omega}^{(b)2}_i \tilde{q}^{(b)2}_i\right] + \tilde{c}^{(b)}_i \tilde{q}^{(b)}_i |H\rangle\langle H|\right\},$$

where $\tilde{q}_i$ are the transformed coordinate (containing both Q_b and q_i) and they form a bath with a Brownian spectral density from which $\tilde{c}_i$ is sampled:

$$\begin{aligned} j_{brown}(\omega) &= \frac{C_b^2\gamma\omega}{\left(\omega^2 - \Omega_b^2\right)^2 + \gamma^2\omega^2} = \frac{2S\Omega_b^3\gamma\omega}{\left(\omega^2 - \Omega_b^2\right)^2 + \gamma^2\omega} \\ &= \frac{2\lambda_b\Omega_b^2\gamma\omega}{\left(\omega^2 - \Omega_b^2\right)^2 + \gamma^2\omega^2}, \end{aligned} \tag{A12}$$

where $j_{brown}(\omega) = \frac{\pi}{2}\sum_i^{\tilde{n}}\frac{\tilde{c}^{(b)2}_i}{\tilde{\omega}^{(b)}_i}\delta(\omega - \tilde{\omega}^{(b)}_i)$. Here we define the solvent reorganization energy as $\lambda_b = S\Omega_b$. In the case where $\gamma \gg 2\Omega_b$, the Brownian spectral density can be rewritten as $j(\omega) = \frac{2\lambda_b\Gamma_b\omega}{\omega^2+\Lambda_b^2}$ which is the Debye cutoff ohmic spectral density, with $\Gamma_b = \Omega_b^2/\gamma$ (and $\tau_b = 1/\Gamma_b$ is the solvent response time). This is the so-called over-damped Brownian oscillator model,[45] which is a special case of the Brownian model. In the reaction center application, the explicit Brownian oscillator does not obey this relation due the parameters being appropriate for the under-damped limit with $\gamma < \Omega_b$. In the

reaction center model, due to the initial phase shift of the Brownian oscillator coordinate, it is better to use the Brownian oscillator model rather than the transformed form since the non-thermal initial condition is hard to transform for the $\hat{H}^{brown}_{trans}$ representation. Alternatively, we can set up the Brownian oscillator model by integrating out the dissipative bath degrees of freedoms giving an influence functional form for the Brownian mode, which can be modeled using a quantum Langevin like dynamics.[46] Here, however, we simply use the ILDM scheme[35] to explicitly propagate every degree of freedom for the bath, including the dissipative bath oscillators coupled to Brownian mode.

The top panels of Fig. 5 present the site population ρ_{HH} for the initial condition of the Brownian oscillator with phase shift $\phi = 0.28$ using initial conditions (1) and (2). These upper panels also compare results with, or with out the Brownian mode, which is seen to provide simply a low frequency modulation on the high frequency electronic population oscillation. From the left and right panels we see that for the model without the additional Brownian mode and its dissipative bath, the population simply oscillates with a period of about 40 fs. This frequency is determined by electronic properties (site energy difference and electronic coupling, which determined the behavior of $|H\rangle$ as $|a_H(t)|^2 \sim 1 - 4\cos^2\theta\sin^2\theta\sin^2(\delta t/\hbar)$ where $\delta = \frac{1}{2}\sqrt{[\epsilon_H - \epsilon_B]^2 + 4\Delta^2_{H,B}}$ and $\theta = \frac{1}{2}\{\frac{\pi}{2} - \sin^{-1}([\epsilon_H - \epsilon_B]/2\delta)\}$ (Ref. 36)) and agrees with the behavior observed as the fine structure in the experiment.[1] If we include the $\hat{H}^{brown}$ component, it gives the modulating envelop with a slower oscillation frequency with a period of about 125 fs corresponding to the 250 cm^{-1} Brownian oscillator frequency. This is the major beating frequency observed in the experimental results[1] and originates from some protein environmental vibrational degree of freedom being excited during the experiment. Also we observe that the electronic beating damps out at about 120 fs if no bath correlation effects are included ($a = 0$). This is much shorter than the experimentally observed decoherence time scale around 300 fs, suggesting the importance of correlated bath motions. Thus, one way to capture the experimentally observed longer decoherence time, is to include correlated fluctuations in site energies driven by the environment. However, such correlated site energy fluctuations have not been observed in detailed simulations. The main text of this paper suggests that correlations in off-diagonal couplings, that have been observed in model system studies, may lead to long coherence times with

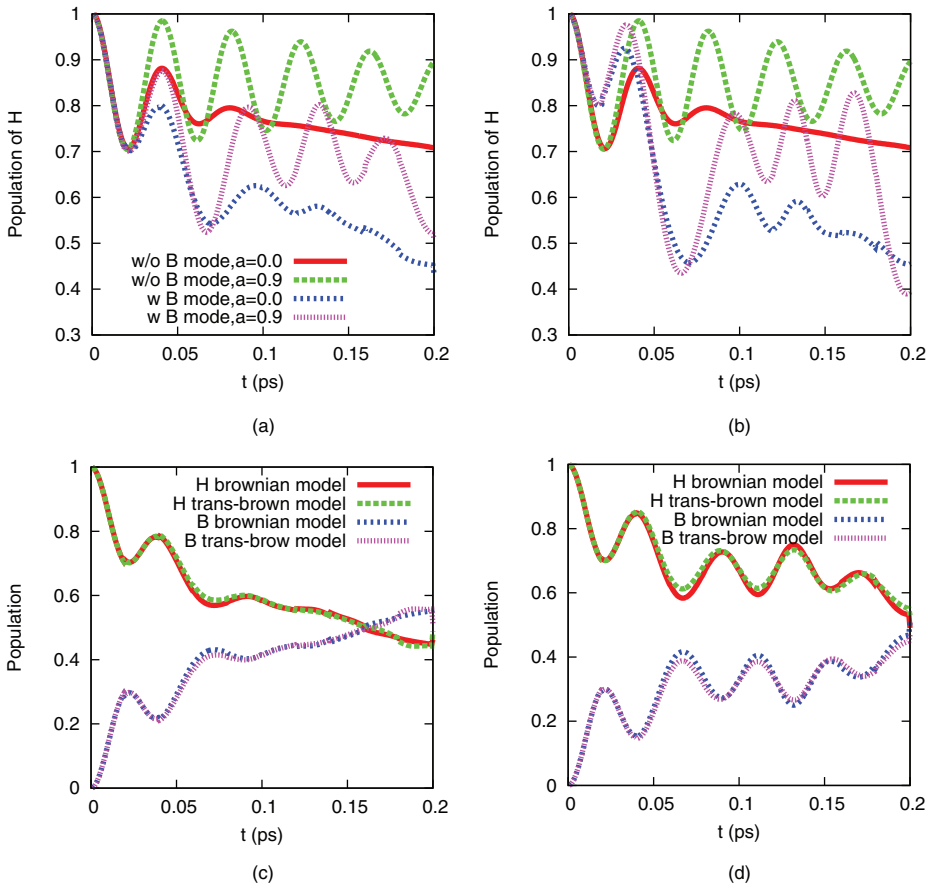

FIG. 5. Top panels: Population of H at $T = 180$ K with initial excitation at H. The site disorders are 20 cm^{-1} for both B and H. Left panel: Q_b sampled from Wigner density $Tr_{P_b}\rho_w \sim \tanh(\beta\Omega_b/2)e^{[-\tanh(\beta\Omega_b/2)/\Omega_b][(\Omega_b^2 Q_b^2/2)]}$ and $P_b = \tan\phi Q_b$. Right panel: $Q_b = \sqrt{\frac{1}{\Omega_b}}\cos\phi$, $P_b = \sqrt{\Omega_b}\sin\phi$. Bottom panels: Population of H and B for initial condition which has the thermal distribution of the Brownian mode, i.e., $\rho_w = \tanh(\beta\Omega_b/2)e^{-[\tanh(\beta\Omega_b/2)\Omega_b][P_b^2/2+(\Omega_b^2 Q_b^2/2)]}$. Left panel is the situation for $a = 0$ and right for $a = 0.9$. Also the results for both Brownian oscillator model and system-bath coupling model with a Brownian spectral density are presented. Red and greed curves are H and B populations obtained from the Brownian oscillator model, and blue and magenta curves are H and B populations obtained from the system-bath model.

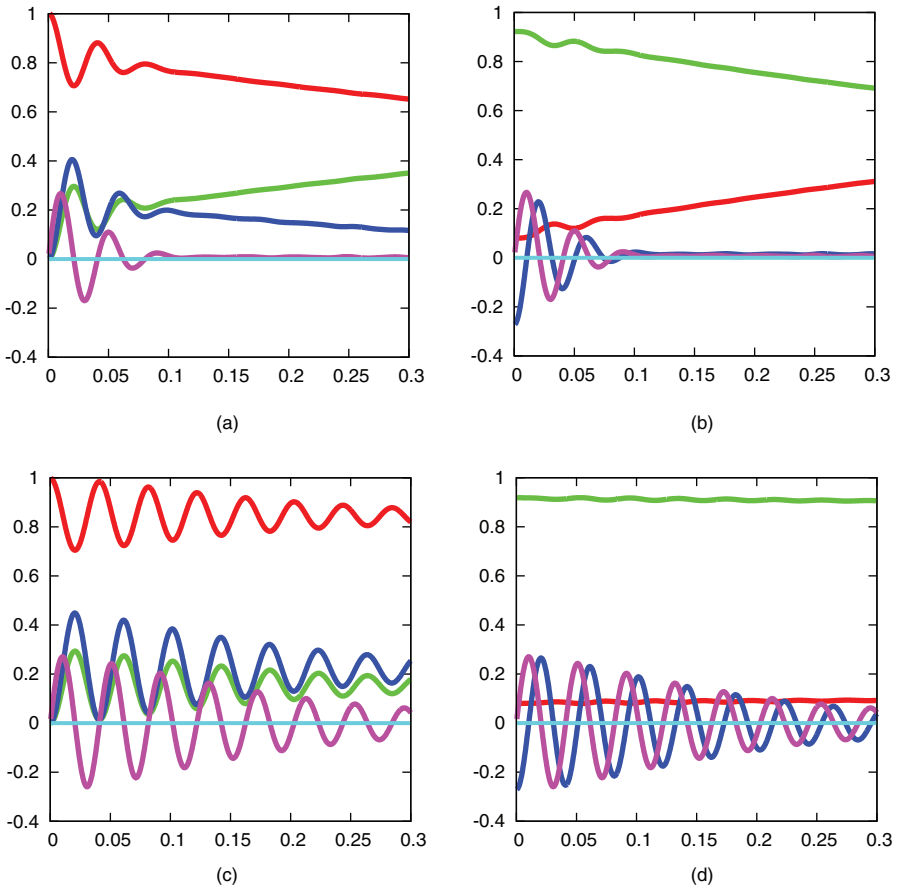

FIG. 6. Dynamics of the reaction center model that ignores the $\hat{H}^{brown}$ part of the Hamiltonian. Initially the excitation is localized at state H, $T = 180$ K. The time axis in this figure is given in picoseconds. Top panels: $a = 0$, bottom panels: $a = 0.9$. Left panels give results in the site basis set ($|H\rangle$ and $|B\rangle$): ρ_{HH}, ρ_{BB}, $\mathrm{Re}\rho_{HB}$, $\mathrm{Im}\rho_{HB}$ are represent by red, green, blue, and magenta curves, respectively. Right panels give results in exciton basis set ($|+\rangle$ and $|-\rangle$), and ρ_{++}, ρ_{--}, $\mathrm{Re}\rho_{+-}$, $\mathrm{Im}\rho_{+-}$ are represent by red, green, blue, and magenta curves, respectively.

different, perhaps experimentally distinguishable, dynamical characteristics.

The dynamics for Brownian model with the thermal initial distribution (initial condition 3) is presented in bottom panels of Fig. 5 with $a = 0$ (left) or $a = 0.9$ (right) spatial correlation. Due to the thermal distribution of all degrees of freedom, the Brownian oscillator model $\hat{H}^{brown}$ and the system-bath transformed Brownian model $\hat{H}^{brown}_{trans}$ with a Brownian spectral density give exactly same reduced density matrix dynamics. Populations for H and B obtain from both models are compared.

Finally, in Fig. 6 we use the reaction center model in the absence of the Brownian mode to explore the effects of correlations in site energy fluctuations on decoherence time and the representation dependence of decoherence terms in the density matrix. In the top left panel ($a = 0$), we see the real part of the coherence ρ_{HB} maintains a finite amplitude at long times A detail explanation of this phenomenon is provided in Ref. 36 in terms of the overlaps of the time dependent environmental wave packets. The right panels show the results in exciton basis set ($|+\rangle$ and $|-\rangle$, which are the eigenstates of $\hat{H}_S$). Bottom panels compare site and exciton basis results: $\rho_{HH} - \rho_{BB}$, $2|\rho_{HB}|$, $\rho_{++} - \rho_{--}$, $2|\rho_{+-}|$ are represent by red, green, blue, and magenta curves. One can see that the real part of coherence in site basis which maintains finite value at long times, vanishes at exciton basis. This is an example of representation dependence of the "coherence." The life time of the oscillations in the coherence matrix elements is universal (i.e., will always exist in either representation).

[1]H. Lee, Y.-C. Cheng, and G. R. Fleming, Science **316**, 1462 (2007).
[2]E. Collini, C. Y. Wong, K. E. Wilk, P. M. G. Curmi, P. Brumer, and G. D. Scholes, Nature (London) **463**, 644 (2010).
[3]G. S. Engel, T. R. Calhoun, E. L. Read, T.-K. Ahn, T. Mancal, Y.-C. Cheng, R. E. Blankenship, and G. R. Fleming, Nature (London) **446**, 782 (2007); G. Panitchayangkoona, D. Hayes, K. A. Fransted, J. R. Caram, E. Harel, J. Wen, R. E. Blankenship, and G. S. Engel, Proc. Natl. Acad. Sci. U.S.A. **107**, 12766 (2010).
[4]T. R. Calhoun, N. S. Ginsberg, G. S. Schlau-Cohen, Y.-C. Cheng, M. Ballottari, R. Bassi, and G. R. Fleming, J. Phys. Chem. B **113**, 16291 (2009).
[5]A. Ishizaki, T. R. Calhoun, G. S. Schlau-Cohenab, and G. R. Fleming, Phys. Chem. Chem. Phys. **12**, 7319 (2010).
[6]E. Collini and G. D. Scholes, Science **323**, 369 (2009).
[7]N. Demirdöven, M. Khalil, and A. Tokmakoff, Phys. Rev. Lett. **89**, 237401 (2002); J. Phys. Chem. A. **107**, 5258 (2003).
[8]A. Ishizaki and Y. Tanimura, J. Phys. Chem. A **111**, 9296 (2007).
[9]A. G. Dijkstra and Y. Tanimura, New J. Phys. **12**, 055005 (2010).
[10]T. Kubař, U. Kleinekathöfer, and M. Elstner, J. Phys. Chem. B **113**, 13107 (2009).
[11]C. Olbrich, J. Strümpfer, K. Schulten, and U. Kleinekathöfer, J. Phys. Chem. B **115**, 758 (2011).
[12]S. Shim, P. Rebentrost, S. Valleau, and A. Aspuru-Guzik, Biophys. J. **102**, 649 (2012).
[13]C. Olbrich and U. Kleinekathöfer, J. Phys. Chem. B **114**, 12427 (2010).

[14]Y. Jing, R. Zheng, H.-X. Li, and Q. Shi, J. Phys. Chem. B **116**, 1164 (2012).
[15]C. Curutchet, J. Kongsted, A. Muñoz-Losa, H. Hossein-Nejad, G. D. Scholes, and B. Mennucci, J. Am. Chem. Soc. **133**, 3078 (2011).
[16]J. Adolphs and T. Renger, Biophys. J. **91**, 2778 (2006).
[17]M. Sarovar, Y.-C. Cheng, and K. B. Whaley, Phys. Rev. E **83**, 011906 (2011).
[18]P. Rebentrost, M. Mohseni, and A. Aspuru-Guzik, J. Phys. Chem. B **113**, 9942 (2009).
[19]J. Wu, F. Liu, Y. Shen, J. Cao, and R. J. Silbey, New J. Phys. **12**, 105012 (2010).
[20]P. Nalbach, J. Eckel, and M. Thorwart, New J. Phys. **12**, 065043 (2010); P. Nalbach and M. Thorwart, New J. Phys. **11**, 085001 (2009); New J. Phys. **12**, 194111 (2010).
[21]F. Fassioli, A. Nazir, and A. Olaya-Castro, J. Phys. Chem. Lett. **1**, 2139 (2010); F. Fassioli and A. Olaya-Castro, New J. Phys. **12**, 085006 (2010).
[22]D. Abramavicius and S. Mukamel, J. Chem. Phys. **134**, 174504 (2011).
[23]A. Ishizaki and G. R. Fleming, New J. Phys. **12**, 055004 (2010).
[24]S. Jang, J. Chem. Phys. **131**, 164101 (2009); S. Jang, Y.-C. Cheng, D. R. Reichman, and J. D. Eaves, J. Chem. Phys. **129**, 101104 (2008).
[25]E. Hennebicq, D. Beljonne, C. Curutchet, G. D. Scholes, and R. J. Silbey, J. Chem. Phys. **130**, 214505 (2009).
[26]J. Strümpfer and K. Schulten, J. Chem. Phys. **134**, 095102 (2011).
[27]S. Jang, J. Chem. Phys. **127**, 174710 (2007).
[28]X. Chen and R. J. Silbey, J. Chem. Phys. **132**, 204503 (2010).
[29]S. M. Vlaming and R. J. Silbey, J. Chem. Phys. **136**, 055102 (2012).
[30]W. R. Cook, R. D. Coalson and D. G. Evans, J. Phys. Chem. B **113**, 11437 (2009).
[31]R. Hernandez and G. A. Voth, Chem. Phys. **223**, 243 (1998); J. A. Poulsen, G. Nyman, and P. J. Rossky, J. Chem. Phys. **119**, 12179 (2003); J. A. Poulsen and G. Nyman, J. Phys. Chem. A **108**, 8743 (2004); J. A. Poulsen, G. Nyman, and P. J. Rossky, Proc. Natl. Acad. Sci. **102**, 6709 (2005); Q. Shi and E. Geva, J. Phys. Chem. A **107**, 9059 (2003); Q. Shi and E. Geva, J. Chem. Phys. **118**, 8173 (2003); Q. Shi and E. Geva, J. Chem. Phys. **119**, 9030 (2003); Q. Shi and E. Geva, J. Chem. Phys. **118**, 7562 (2003).
[32]Z. Ma and D. F. Coker, J. Chem. Phys. **128**, 244108 (2008).
[33]W. H. Miller and C. W. McCurdy, J. Chem. Phys. **69**, 5163 (1978); H. D. Meyer and W. H. Miller, J. Chem. Phys. **70**, 3214 (1979); G. Stock and M. Thoss, Phys. Rev. Lett. **78**, 578 (1997); M. Thoss and G. Stock, Phys. Rev. A **59**, 64 (1999); S. Bonella, and D. F. Coker, J. Chem. Phys. **114**, 7778 (2001); S. Bonella and D. F. Coker, J. Chem. Phys. **118**, 4370 (2003).
[34]P. Huo and D. F. Coker, J. Chem. Phys. **135**, 201101 (2011).
[35]E. R. Dunkel, S. Bonella, and D. F. Coker, J. Chem. Phys. **129**, 114106 (2008); S. Bonella and D. F. Coker, J. Chem. Phys. **122**, 194102 (2005); S. Bonella, D. Montemayor, and D. F. Coker, Proc. Natl. Acad. Sci. U.S.A. **102**, 6715 (2005).
[36]P. Huo and D. F. Coker, J. Chem. Phys. **133**, 184108 (2010).
[37]P. Huo and D. F. Coker, J. Phys. Chem. Lett. **2**, 825 (2011).
[38]S. Jang, M. D. Newton, and R. J. Silbey, Phys. Rev. Lett. **92**, 218301 (2004); Y.-C. Cheng and R. J. Silbey, Phys. Rev. Lett. **96**, 028103 (2006); S. Jang, M. D. Netwton, and R. J. Silbey, J. Phys. Chem. B **111**, 6807 (2007).
[39]See supplementary material at http://dx.doi.org/10.1063/1.3693019 for: (1) outline of PLDM approach, and (2) summary of the Haken-Strobl model and the Liouville matrix for the three state model considered here.
[40]C. P. Hsu, G. R. Fleming, M. Head-Gordon, and T. Head-Gordon, J. Chem. Phys. **114**, 3065 (2001); R. Metivier, F. Nolde, K. Muellen, and T. Basche, Phys. Rev. Lett. **98**, 047802 (2007); D. J. Heijs, V. A. Malyshev, and J. Knoester, Phys. Rev. Lett. **95**, 177402 (2005); M. Schroder, U. Kleinekathofer, and M. Schreiber, J. Chem. Phys. **124**, 084903 (2006); B. Palmieri, D. Abramavicius, and S. Mukamel, J. Chem. Phys. **130**, 204512 (2009); D. Abramavicius, and S. Mukamel, J. Chem. Phys. **133**, 064510 (2010); A. Olaya-Castro, C. Fan-Lee, F. Fassioli-Olsen, and N. F. Johnson, Phys. Rev. B **78**, 085115 (2008); X. J. Yang, T. E. Dykstra, and G. D. Scholes, Phys. Rev. B **71**, 045203 (2005); M. N. Yang, J. Chem. Phys. **123**, 124705 (2005); Y. C. Cheng and R. J. Silbey, J. Phys. Chem. B. **109**, 21399 (2005); A. Ishizaki and G. R. Fleming, J. Chem. Phys. **130**, 234110 (2009).
[41]A. Ishizaki and G. R. Fleming, J. Chem. Phys. **130**, 234111 (2009); G. Tao and W. H. Miller, J. Phys. Chem. Lett. **1**, 891 (2010); R. Chakraborty, P. Rebentrost, and A. Aspuru-Guzik, J. Chem. Phys. **131**, 184102 (2009); A. Kelly and Y. M. Rhee, J. Phys. Chem. Lett. **2**, 808 (2011).
[42]A. Ishizaki and G. R. Fleming, Proc. Natl. Acad. Sci. U.S.A. **106**, 17255 (2009).
[43]N. Makri, E. J. Sim, D. E. Makarov, and M. Topaler, Proc. Natl. Acad. Sci. U.S.A. **93**, 3926 (1996); E. Sim and N. Makri, J. Phys. Chem. B **101**, 5446 (1997).
[44]A. Garg, J. N. Onuchic, and V. Ambegaokar, J. Chem. Phys. **83**, 4491 (1985); J. Cao and G. A. Voth, J. Chem. Phys **106**, 1769 (1997); J. Cao, J. Chem. Phys **107**, 3204 (1997); K. H. Hughes, C. D. Christ, and I. Burghardt, J. Chem. Phys. **131**, 024109 (2009).
[45]S. Mukamel, *Principles of Nonlinear Optical Spectroscopy* (Oxford University Press, New York, 1995).
[46]P. Huo, S. Bonella, L. Chen, and D. F. Coker, Chem. Phys. **370**, 87 (2010).
[47]M. Sarovar, A. Ishizaki, G. R. Fleming, and K. B. Whaley, Nat. Phys. **6**, 462 (2010).
[48]D. Hayes, G. Panitchayangkoon, K. A. Fransted, J. R. Caram, J. Wen, K. F. Freed, and G. S. Engel, New J. Phys. **12**, 065042 (2010).
[49]J. Cao and R. J. Silbey, J. Phys. Chem. A **113**, 13826 (2009).
[50]F. Caruso, A. W. Chin, A. Datta, S. F. Huelga, and M. B. Plenio, J. Chem. Phys **131**, 105106 (2009); M. B. Plenio and S. F. Huelga, New J. Phys **10**, 113019 (2008); F. Caruso, A. W. Chin, A. Datta, S. F. Huelga, and M. B. Plenio, Phys. Rev. A. **81**, 062346 (2010); A. W. Chin, A. Datta, F. Caruso, S. F. Huelga and M. B. Plenio, New J. Phys **12**, 065002 (2010).
[51]S. Bonella and D. F. Coker, J. Chem. Phys. **118**, 4370 (2003).
[52]J. Yuen-Zhou and A. Aspuru-Guzik, J. Chem. Phys. **134**, 134505 (2011).
[53]For simplicity, throughout we use this classical relationship between the correlation functions and the corresponding spectral densities. Switching to the quantum expression will not influence the results presented here since we use the spectral density directly, not the correlation function, and both quantum and classical expression maintain the linear relationship between correlation function function and spectral density.